

INFORMATION TO USERS

This manuscript has been reproduced from the microfilm master. UMI films the text directly from the original or copy submitted. Thus, some thesis and dissertation copies are in typewriter face, while others may be from any type of computer printer.

The quality of this reproduction is dependent upon the quality of the copy submitted. Broken or indistinct print, colored or poor quality illustrations and photographs, print bleedthrough, substandard margins, and improper alignment can adversely affect reproduction.

In the unlikely event that the author did not send UMI a complete manuscript and there are missing pages, these will be noted. Also, if unauthorized copyright material had to be removed, a note will indicate the deletion.

Oversize materials (e.g., maps, drawings, charts) are reproduced by sectioning the original, beginning at the upper left-hand corner and continuing from left to right in equal sections with small overlaps. Each original is also photographed in one exposure and is included in reduced form at the back of the book.

Photographs included in the original manuscript have been reproduced xerographically in this copy. Higher quality 6" x 9" black and white photographic prints are available for any photographs or illustrations appearing in this copy for an additional charge. Contact UMI directly to order.

U·M·I

University Microfilms International
A Bell & Howell Information Company
300 North Zeeb Road, Ann Arbor, MI 48106-1346 USA
313/761-4700 800/521-0600

Order Number 1343846

**Automatic development of circuit and interconnection equations
on the basis of topology and library of network components:
SPICE approach**

Lee, Dongjin, M.S.

The University of Arizona, 1991

U·M·I
300 N. Zeeb Rd.
Ann Arbor, MI 48106

**AUTOMATIC DEVELOPMENT OF CIRCUIT AND INTERCONNECTION
EQUATIONS ON THE BASIS OF TOPOLOGY AND LIBRARY
OF NETWORK COMPONENTS - SPICE APPROACH**

by

Dongjin Lee

**A Thesis Submitted to the Faculty of the
DEPARTMENT OF ELECTRICAL AND COMPUTER ENGINEERING
In Partial Fulfillment of the Requirements
For the Degree of
MASTER OF SCIENCE
WITH A MAJOR IN ELECTRICAL ENGINEERING
In the Graduate College
THE UNIVERSITY OF ARIZONA**

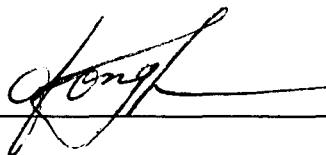
1991

STATEMENT BY AUTHOR

This thesis has been submitted in partial fulfillment of requirement for an advanced degree at The University of Arizona and is deposited in the University Library to be made available to borrowers under rules of the Library.

Brief quotations from this thesis are allowable without special permission, provided that accurate acknowledgment of source is made. Requests for permission for extended quotation from or reproduction of this manuscript in whole or in part may be granted by the head of the major department or the Dean of the Graduate College when in his or her judgment the proposed use of the material is in the interests of scholarship. In all other instances, however, permission must be obtained from the author.

SIGNED: _____

A handwritten signature in cursive script, appearing to read 'Kong', written over a horizontal line.**APPROVAL BY THESIS DIRECTOR**

This thesis has been approved on the date shown below:

Olgiard A. Palusinski
Dr. Olgiard A. Palusinski
Professor of Electrical and Computer Engineering.

April 25, 1991
Date

ACKNOWLEDGMENTS

I wish to express my gratitude for the encouragement and guidance of my advisor, Dr. Olgierd A. Palusinski, whose help made this thesis possible. I would like to thank Dr. Andreas C. Cangellaris, reviewer of this thesis, for his comments and suggestions concerning its final text.

I am also thankful to my wife; Sung-Mi, my two children; Kibuom, Kihyun, my parents, my parents-in-laws, and all my family for their painful endurance and devoted support.

I give special thanks to Dae-Eu Kim for financial support and my friend, Jiseung Nam, for discussing the computer program.

This work was supported in part by the NSF grant: MIP-9017037 and in part the University of Arizona fund #233010 (VIDEOCAMPUS discretionary).

TABLE OF CONTENTS

		Page
	LIST OF ILLUSTRATIONS	6
	LIST OF TABLES	8
	ABSTRACT	9
CHAPTER		
1.	INTRODUCTION	10
2.	MODELING OF MULTI-CONDUCTOR LOSSLESS TRANSMISSION LINES	13
	2.1 Coupled Lossless Transmission Line Equations	13
	2.2 Equivalent Circuit of an N-Conductor Lossless Transmission Line	20
3.	NUMERICAL ALGORITHM	24
	3.1 Modified Nodal Analysis of Lossless Transmission Lines	24
	3.2 DC Analysis	27
	3.3 Tracking of wave propagation	28
	3.4 Procedure for the Transient Analysis	33
4.	COMPUTER IMPLEMENTATION WITH THE USE OF SPICE PROGRAM	37
	4.1 Input Format	37
	4.2 Block Diagram of LSPICE	38
	4.3 Linked list specification	40
	4.4 Element Load Structure	43
	4.5 Application of Input Processing Module	44
	4.6 Application of Interconnection Equation Module	45

TABLE OF CONTENTS--Continued

CHAPTER	Page
5.	NUMERICAL EXPERIMENTS 48 5.1 Simulation of a Linear Network Containing One Transmission Line System 48 5.2 Simulation of a Linear Network Containing Two Transmission Line Systems 56 5.3 Simulation of a Nonlinear Network with One Transmission Line 65 5.4 Simulation of a Nonlinear Network with Two Transmission Lines 73
6.	CONCLUSIONS 81 APPENDIX A: INPUT FILES FOR EXAMPLES USED IN NUMERICAL EXPERIMENTS 83 APPENDIX B: COMMON STATEMENTS 86 LIST OF REFERENCES 88

LIST OF ILLUSTRATIONS

Figure	Page
2.1.1 An N-Conductor Transmission Line	13
2.2.1 Equivalent Circuit of an N-Conductor Lossless Transmission Line	20
3.1.1 Modified Nodal Equation Matrix for Coupled Lossless Transmission Lines - entries related m^{th} Conductor	25
3.1.2 Modified Nodal Equation Matrix for Characteristic Admittance Matrix	26
3.3.1 Discretization of Modal Wave	31
a) Left Traveling Wave at Left Boundary ($x=0$)	
b) Right Traveling Wave at Right Boundary ($x=d$)	
4.2.1 Block Diagram of LSPICE	39
5.1.1 A Linear Network containing a Two-Conductor Transmission Line System	49
5.1.2 Driving Voltage of the Network in Fig. 5.1.1	50
5.1.3 Transient Response calculated by LSPICE with $\text{RELTOL}=10^{-4}$	51
A: Voltage at node 2; B: Voltage at node 3;	
C: Voltage at node 4; D: Voltage at node 5.	
5.1.4 Transient Response calculated by UANTL with $\text{ETOL}=10^{-4}$	52
A: Voltage at node 2; B: Voltage at node 3;	
C: Voltage at node 4; D: Voltage at node 5.	
5.2.1 A Linear Network containing Two Transmission Line Systems	56
5.2.2 Driving Voltage of the Network in Fig. 5.2.1	57
5.2.3 Transient Response calculated by LSPICE with $\text{RELTOL}=10^{-4}$	58
A: Voltage at node 2; B: Voltage at node 3;	
C: Voltage at node 11; D: Voltage at node 12.	
5.2.4 Transient Response calculated by UANTL with $\text{ETOL}=10^{-4}$	59
A: Voltage at node 2; B: Voltage at node 3;	
C: Voltage at node 11; D: Voltage at node 12.	

LIST OF ILLUSTRATIONS--Continued

Figure	Page
5.2.5 Transient Response calculated by LSPICE with RELTOL= 10^{-4} A: Voltage at node 2; B: Voltage at node 11.	60
5.2.6 Transient Response calculated by UANTL with ETOL= 10^{-4} A: Voltage at node 2; B: Voltage at node 11.	61
5.3.1 A Nonlinear Network with One Transmission Line	65
5.3.2 Driving Voltage of the Network in Fig. 5.3.1	66
5.3.3 Transient Response calculated by LSPICE with RELTOL= 10^{-4} A: Voltage at node 2; B: Voltage at node 3; C: Voltage at node 8; D: Voltage at node 9.	68
5.3.4 Transient Response calculated by UANTL with ETOL= 10^{-4} A: Voltage at node 2; B: Voltage at node 3; C: Voltage at node 8; D: Voltage at node 9.	69
5.4.1 A Nonlinear Network with Two Transmission lines	73
5.4.2 Transient Response calculated by LSPICE with RELTOL= 10^{-4} A: Voltage at node 2; B: Voltage at node 3; C: Voltage at node 11; D: Voltage at node 15.	75
5.4.3 Transient Response calculated by UANTL with ETOL= 10^{-4} A: Voltage at node 2; B: Voltage at node 3; C: Voltage at node 11; D: Voltage at node 15.	76

LIST OF TABLES

Table	Page
5.1.1 Percentage Error of Voltage at Node 4 from the Reference Value	54
5.1.2 Percentage Error of Voltage at Node 5 from the Reference Value	55
5.2.1 Percentage Error of Voltage at Node 2 from the Reference Value	63
5.2.2 Percentage Error of Voltage at Node 11 from the Reference Value	64
5.3.1 Percentage Error of Voltage at Node 8 from the Reference Value	71
5.3.2 Percentage Error of Voltage at Node 9 from the Reference Value	72
5.4.1 Percentage Error of Voltage at Node 11 from the Reference Value	78
5.4.2 Percentage Error of Voltage at Node 15 from the Reference Value	79

ABSTRACT

The modules for processing of interconnection specifications which are provided in an input file of circuit analyzer were developed. A software package for creation of appropriate computer models on the basis of topology and library of network components was also constructed and implemented using SPICE program. A computer program, called LSPICE, has been developed by combining SPICE numerical techniques and the modal analysis of coupled transmission lines. This program can be used for simulating the transient response of networks containing coupled lossless transmission lines. Several example networks have been simulated using this program. The results have been compared with those generated by the circuit simulator program called UANTL. The LSPICE has several advantages over UANTL and SPICE in simulating the transient response of network containing coupled lossless transmission lines. A description of LSPICE and a summary of the results of numerical experiments are included.

CHAPTER 1

INTRODUCTION

Studying development of simulators it may be noticed that whenever a new circuit simulator was developed, a new input processing module was also written. A development of input processor takes a relatively large amount of time. Also, it usually appears that developer did not think that it was worthwhile to spend more than a minimum of effort on constructing the input processing part of the simulation program. Consequently, an input processing is usually implemented in an unsatisfying way. It is therefore desirable to develop a general and efficient input processing software which can be used to form equations of any circuit including coupled transmission lines. With the increase of signal speed and growth of interconnection density on a chip and on a circuit board, transmission line behavior has become an important issue in the design of electronic systems and packages. Reflection, propagation delay, dispersion, and crosstalk are the problems related to transmission lines. They cause signal distortion and may even result in malfunctioning of an electronic system.

The principal way of obtaining information about the effect of coupled transmission lines on a system performance is by analyzing the transient response at the predetermined nodes of the system. Such analysis is extremely complicated and must be done with the aid of computer simulation. The methods for simulation of circuit networks are well developed and widely used in practice in the form of various versions of SPICE program (University of California, Berkely). Also, input format of SPICE is well-known because it works with alphanumeric, descriptive elements rather than pure digits or numbers. Unfortunately,

available versions of SPICE allow for simulation of decoupled transmission lines only. Simulation of coupled transmission lines with SPICE faces serious difficulties such as determination of number of lumped cells which must be used to represent the coupled transmission lines and construction of the equivalent circuit of coupled transmission line system. UANTL program (Liao, 1989; Palusinski, et al., 1990) can be used for simulating the transient response of linear and nonlinear networks with coupled lossless transmission lines, but its input file format differs from that of SPICE, which precludes the processing of wide variety of existing SPICE circuit models. The UANTL input format is also more difficult to use, because it uses numerical codes for definition of network components in place of alphanumeric ones which are much easier to remember and use. Another limitation of UANTL is the fact that it has built in simplest device models only. It does not have newer transistor models such as MOSFET level 2 model which portrays short channel effects so important in contemporary IC technologies.

This work can be summarized as follows. From the circuit description provided in the input file, a unified internal representation (UIR) of the circuit is generated. Input processing of a simulator consists of modules which are used like library functions with a tool concept. Because input processing will be often used in different applications, it was decided to make an effort of writing a possibly general and efficient software package. It was assumed that input processing should be able to process SPICE input files. Initially, only a subset of SPICE's input language might be allowed. The UIR should be a complete representation of the circuit including the information needed for analysis and output. The UIR should be independent of analysis algorithm. Composite elements should be expanded into equivalent circuits. Major task of input processing is to read the input file, check for

formal-syntactic errors, and rewrite the information in a way convenient for further processing by simulation software like for example constructing the modified nodal equation matrix.

A lossless multi-conductor transmission line is replaced by two equivalent circuits, one at each end of the transmission line. The equivalent circuits are composed of resistive networks and time varying voltage controlled voltage sources (VCVS in a circuit jargon) which depend on wave propagation between the two ends of the transmission line. Modified nodal analysis (MNA) with general circuit variables is used to obtain computer model of network of lumped circuits with coupled transmission line systems.

A computer program, called LSPICE, has been developed by combining SPICE and the modal analysis of coupled transmission lines. This program can be used for simulating the transient response of networks containing coupled lossless transmission lines. A program for processing of input files describing circuits and interconnections, called SIP, has been developed during the course of this work. This program can be used as a library function or as a tool for processing of input files containing a description of networks with coupled lossless transmission lines.

CHAPTER 2

MODELING OF MULTI-CONDUCTOR LOSSLESS
TRANSMISSION LINES

In this chapter, a brief summary of the theoretical background related to transmission lines is presented. Transmission line equations and modal analysis in time domain are discussed in Section 2.1. The equivalent circuit of N-conductor lossless transmission lines is discussed in Section 2.2.

2.1. Coupled Lossless Transmission Line Equations

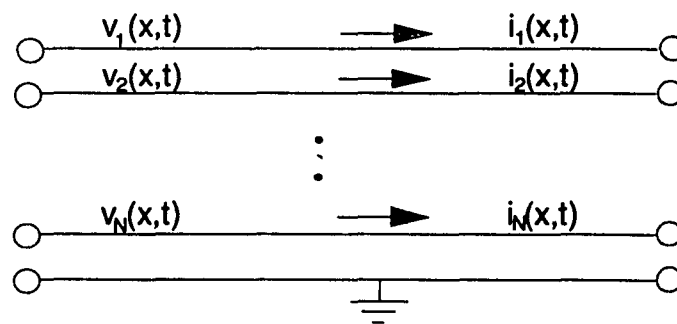


Fig. 2.1.1 An N-Conductor Transmission Line.

A transmission line with N conductors plus one ground conductor is shown in Fig. 2.1.1. The line voltages with respect to the ground, $v_1(x,t), \dots, v_N(x,t)$, and line currents,

$i_1(x,t), \dots, i_N(x,t)$, are defined as indicated in Fig. 2.1.1. We assume here that the dielectrics and conductors are perfect and the cross-sectional dimension of the transmission line is negligibly small compared to the wavelength of the highest significant frequency component involved, so that a transverse electromagnetic (TEM) wave (or quasi-TEM wave) alone propagates (Liao, et al., 1990). Under such assumption, the vectors of line voltages, $\bar{v}(x, t)$, and line currents, $\bar{i}(x, t)$, are related by the following partial differential equations

$$\frac{\partial \bar{v}(x, t)}{\partial x} = -[L] \frac{\partial \bar{i}(x, t)}{\partial t}, \quad (2.1.1)$$

$$\frac{\partial \bar{i}(x, t)}{\partial x} = -[C] \frac{\partial \bar{v}(x, t)}{\partial t}, \quad (2.1.2)$$

where

$$\bar{v}(x, t) = [v_1(x, t), v_2(x, t), \dots, v_N(x, t)]^T, \quad (2.1.3)$$

$$\bar{i}(x, t) = [i_1(x, t), i_2(x, t), \dots, i_N(x, t)]^T. \quad (2.1.4)$$

The superscript T is used here and throughout to indicate the transpose of a matrix or vector. Distance and time are denoted by x and t , respectively, and $[L]$ and $[C]$ are symmetric inductance and capacitance matrices with constant elements, respectively. It can be easily shown that $[L]$ is positive definite matrix with all elements positive and that $[C]$ is a hyperdominant matrix (Ho, 1973). A hyperdominant matrix $[C] = [C_{ij}]$ is a matrix whose elements have the following properties: $C_{ii} > 0, C_{ij} < 0$, and $C_{ii} > \sum_{j \neq i} |C_{ij}|$. The elements of the $[L]$ and $[C]$ matrices can be computed numerically using existing programs (Weeks, 1970; Palusinski, et al., 1987) once the geometries of the lines and the dielectric constants of the insulating materials are specified. The elements of those matrices depend on the geometry and material properties of the interconnecting structure (Weeks, 1970;

Ruehli, 1972).

Equation (2.1.1) and (2.1.2) can be manipulated to obtain the following well known wave equations in time domain:

$$\frac{\partial^2 \bar{v}(x, t)}{\partial x^2} = [L][C] \frac{\partial^2 \bar{v}(x, t)}{\partial t^2}, \quad (2.1.5)$$

$$\frac{\partial^2 \bar{i}(x, t)}{\partial x^2} = [C][L] \frac{\partial^2 \bar{i}(x, t)}{\partial t^2}. \quad (2.1.6)$$

If we now assume that the matrix $[L][C]$ is diagonalizable, we have the relation

$$[L][C] = P\lambda P^{-1}, \quad (2.1.7)$$

where

$$[\lambda] = \begin{bmatrix} \lambda_1 & 0 & \cdot & \cdot & \cdot & 0 \\ 0 & \lambda_2 & \cdot & \cdot & \cdot & 0 \\ \cdot & \cdot & \cdot & \cdot & \cdot & \cdot \\ \cdot & \cdot & \cdot & \cdot & \cdot & \cdot \\ \cdot & \cdot & \cdot & \cdot & \cdot & \cdot \\ 0 & \cdot & \cdot & \cdot & \cdot & \lambda_N \end{bmatrix}. \quad (2.1.8)$$

$[\lambda]$ is the diagonal matrix of eigenvalues. P is $N \times N$ matrix composed of eigenvectors of the matrix $[L][C]$ corresponding to λ_i . P is the identity matrix for structures with homogeneous medium and a full matrix for structures with multilayer dielectrics (Ho, 1973). The matrices $[L][C]$ and $[C][L]$ have the same eigenvalues (Chang, 1970).

Let $\lambda_i = \tau_i^2$ with both λ_i and τ_i being real positive numbers. With this notation the diagonal matrix (2.1.8) may also be denoted τ^2 , which allows us to write (2.1.7) in the form

$$[LC] = P\tau^2 P^{-1}, \quad (2.1.9)$$

The following definition will be useful in further discussions

$$[LC]^{-\frac{1}{2}} = P \tau P^{-1}. \quad (2.1.10)$$

where τ is a diagonal matrix containing the entries $\tau_i = \sqrt{\lambda_i}$.

Substituting (2.1.9) into (2.1.5)

$$\frac{\partial^2 \bar{v}(x, t)}{\partial x^2} = P \tau^2 P^{-1} \frac{\partial^2 \bar{v}(x, t)}{\partial t^2}, \quad (2.1.11)$$

and multiplying the system by P^{-1} from the left we obtain

$$\frac{\partial^2}{\partial x^2} (P^{-1} \bar{v}(x, t)) = \tau^2 \frac{\partial^2}{\partial t^2} (P^{-1} \bar{v}(x, t)). \quad (2.1.12)$$

If we now assume that conditions exist for a transverse electromagnetic (TEM) solution for the line voltage, we have the relation

$$P^{-1} \bar{v}(x, t) = \bar{u}_+(t - \tau x) + \bar{u}_-(t + \tau x), \quad (2.1.13)$$

where τ is the time of wave propagation per unit length (Ho, 1973; Chang, 1987). The symbols $\bar{u}_+(t - \tau x)$ and $\bar{u}_-(t + \tau x)$ represent vectors of modal waves traveling respectively in the positive and the negative direction of the x axis. An explanation of symbols is needed here. Each modal component travels with its own specific velocity $\frac{1}{\tau}$. This means that the modal waves can be represented as follows:

$$\bar{u}_+(t - \tau x) = \begin{pmatrix} u_1(t - \tau_1 x) \\ u_2(t - \tau_2 x) \\ \vdots \\ u_N(t - \tau_N x) \end{pmatrix}_+, \quad (2.1.14)$$

$$\bar{u}_-(t + \tau x) = \begin{pmatrix} u_1(t + \tau_1 x) \\ u_2(t + \tau_2 x) \\ \vdots \\ u_N(t + \tau_N x) \end{pmatrix}_-. \quad (2.1.15)$$

It is thus clear that the speed of propagation (modal velocity, c_i) and the time of propagation per unit length are related to the eigenvalues λ_i of the matrix $[L][C]$ as follows:

$$\begin{aligned} \tau_i &= \sqrt{\lambda_i} \\ &= \frac{1}{c_i} \quad i = 1, 2, \dots, N. \end{aligned} \quad (2.1.16)$$

N is the number of coupled lines and the $+, -$ sign implies that the wave can travel in both the positive and negative directions along the x axis. The equation (2.1.13) can be expressed as following:

$$\bar{v}(x, t) = P\bar{u}_+(t - \tau x) + P\bar{u}_-(t + \tau x). \quad (2.1.17)$$

The equation (2.1.1) can be solved for the vector of transmission line currents.

$$\frac{\partial \bar{i}(x, t)}{\partial t} = -[L]^{-1} \frac{\partial \bar{v}(x, t)}{\partial x} \quad (2.1.18)$$

which, using (2.1.17), can be written as

$$\frac{\partial \bar{i}(x, t)}{\partial t} = -[L]^{-1} \frac{\partial}{\partial x} (P\bar{u}_+(t - \tau x) + P\bar{u}_-(t + \tau x)). \quad (2.1.19)$$

The equation (2.1.19) yields the following solution:

$$\bar{i}(x, t) = L^{-1} P \tau P^{-1} (P\bar{u}_+(t - \tau x) - P\bar{u}_-(t + \tau x)). \quad (2.1.20)$$

On the basis of (2.1.20), we define the characteristic admittance matrix Y_0 (Ho, 1973; Chang, 1987)

$$Y_0 = L^{-1} P \tau P^{-1} \quad (2.1.21)$$

which, using (2.1.10), can be expressed as follows

$$Y_0 = L^{-1} (LC)^{\frac{1}{2}}. \quad (2.1.22)$$

The characteristic impedance matrix Z_0 is

$$Z_0 = Y_0^{-1} = (LC)^{-\frac{1}{2}} L \quad (2.1.23)$$

or after some simple matrix algebra

$$Z_0 = (LC)^{\frac{1}{2}} C^{-1}. \quad (2.1.24)$$

The equations (2.1.17) and (2.1.20) can be rewritten in the following form:

$$\begin{aligned} \bar{v}(x, t) &= P\bar{u}_+(t - \tau x) + P\bar{u}_-(t + \tau x) \\ &= \bar{v}_+(x, t) + \bar{v}_-(x, t), \end{aligned} \quad (2.1.25)$$

$$\begin{aligned} Y_0^{-1} \bar{i}(x, t) &= P\bar{u}_+(t - \tau x) - P\bar{u}_-(t + \tau x) \\ &= \bar{v}_+(x, t) - \bar{v}_-(x, t), \end{aligned} \quad (2.1.26)$$

$$\bar{i}(x, t) = \bar{i}_+(x, t) - \bar{i}_-(x, t), \quad (2.1.27)$$

where

$$\bar{v}_+(x, t) = P\bar{u}_+(t - \tau x), \quad (2.1.28)$$

$$\bar{v}_-(x, t) = P\bar{u}_-(t + \tau x), \quad (2.1.29)$$

$$\bar{i}_+(x, t) = Y_0\bar{v}_+(x, t), \quad (2.1.30)$$

$$\bar{i}_-(x, t) = Y_0\bar{v}_-(x, t). \quad (2.1.31)$$

We define the modal waves u_+ and u_- as follows:

$$\bar{u}_+(x, t) = \bar{u}_+(t - \tau x), \quad (2.1.32)$$

$$\bar{u}_-(x, t) = \bar{u}_-(t + \tau x). \quad (2.1.33)$$

A transverse electromagnetic(TEM) wave propagating along a transmission line can be expressed as a combination of waves propagating with specific characteristic delay times per unit length. Such waves are called modal waves or briefly modes. The subscript "+" sign denotes the wave traveling in the positive direction of the x axis; the subscript "-" sign denotes the wave traveling in opposite direction. The letter τ_i represents delay time per unit length for the i^{th} modal wave.

2.2. Equivalent Circuit of an N-Conductor Lossless Transmission Line

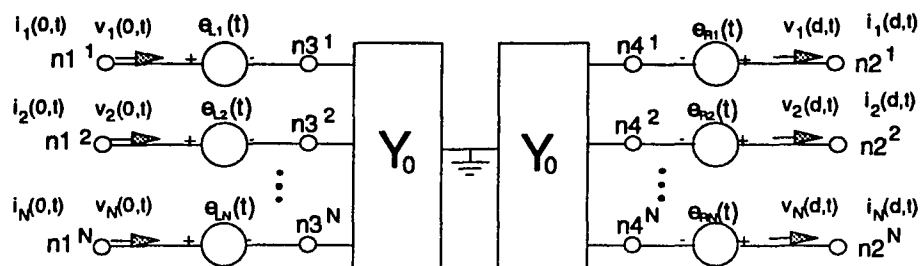


Fig. 2.2.1 Equivalent Circuit of an N-Conductor Lossless Transmission Line

A lossless transmission line can be replaced by equivalent circuits which consists of VCVS and resistive networks as shown in Fig. 2.2.1. The nodes $n1, n2$ are external nodes and the nodes $n3, n4$ are internal nodes of the equivalent circuit of transmission line. The magnitudes of the VCVS, e_{L1}, \dots, e_{LN} and e_{R1}, \dots, e_{RN} , are related to the amplitude of the conductor voltages of the incoming waves at the ends of the transmission line. Tracking the wave propagation along the transmission line, we can determine the magnitudes of the VCVS. The resistive network is the physical realization of the characteristic admittance matrix, $[Y_0]$, of the transmission line. The equivalent circuits contain the same number of VCVS but in addition they need an equal number of current controlled current sources (CCCS) (Chang, 1987). Those sources must be updated at each integration step, and because of this, the equivalent circuits proposed here are computationally more

efficient. The equivalent circuits for transmission lines are incorporated into the terminating networks to form an augmented network which can be analyzed using techniques of network analysis.

From the equivalent circuit in Fig. 2.2.1, we can obtain the following equations

$$\bar{e}_L(t) = \bar{v}(0, t) - Y_0^{-1} \bar{i}(0, t), \quad (2.2.1)$$

$$\bar{e}_R(t) = \bar{v}(d, t) + Y_0^{-1} \bar{i}(d, t), \quad (2.2.2)$$

where $\bar{v}(0, t)$ and $\bar{v}(d, t)$ are vectors of nodal voltages at the left end and the right end of the transmission line, respectively. We substitute (2.1.23), (2.1.24) at $x=0$ and $x=d$ into (2.2.1), (2.2.2), respectively. The amplitude of those sources are twice the amplitudes of the incoming waves at the ends of the transmission line as follows:

$$\begin{aligned} \bar{e}_L(t) &= 2\bar{v}_-(0, t) \\ &= 2P\bar{u}_-(0, t), \end{aligned} \quad (2.2.3)$$

$$\begin{aligned} \bar{e}_R(t) &= 2\bar{v}_+(d, t) \\ &= 2P\bar{u}_+(d, t). \end{aligned} \quad (2.2.4)$$

The modal waveforms in equations, (2.2.3), (2.2.4) have simple traveling wave properties which can be written at each end as follows. For the far end ($x=d$),

$$\bar{u}_+(d, t) = \bar{u}_+(0, t - \tau d), \quad (2.2.5)$$

or using simplified notation (2.1.32)

$$\bar{u}_+(d, t) = \bar{u}_+(t - \tau d). \quad (2.2.6)$$

For the near end ($x=0$),

$$\bar{u}_-(0, t) = \bar{u}_-(d, t - \tau d), \quad (2.2.7)$$

or using simplified notation (2.1.33)

$$\begin{aligned}\bar{u}_-(0,t) &= \bar{u}_-(t) \\ &= \bar{u}_-(t - \tau d + \tau d).\end{aligned}\tag{2.2.8}$$

The notation introduced in (2.2.5),(2.2.6),(2.2.7), and (2.2.8) will be useful in explaining the wave tracking algorithm in the Section 3.3.

At any time instant if we know the amplitudes of the incoming waves at both ends of each transmission line, i.e., $u_-(d,t)$ at the right end and $u_+(0,t)$ at the left end, we can carry out the network analysis and obtain nodal voltages of all network nodes including those at both ends of each transmission line. The line voltages are obtained by summing the incoming voltage wave and the outgoing voltage wave at both ends of each transmission line which yields

$$\bar{v}(0,t) = \bar{v}_+(0,t) + \bar{v}_-(0,t),\tag{2.2.9}$$

$$\bar{v}(d,t) = \bar{v}_+(d,t) + \bar{v}_-(d,t),\tag{2.2.10}$$

Expressing \bar{v}_+ and \bar{v}_- in term of \bar{u}_+ and \bar{u}_- , we obtain from (2.2.3),(2.2.4),(2.2.9), and (2.2.10)

$$\bar{v}_-(0,t) = \bar{v}(0,t) - P\bar{u}_+(0,t),\tag{2.2.11}$$

$$\bar{v}_+(d,t) = \bar{v}(d,t) - P\bar{u}_-(d,t).\tag{2.2.12}$$

Equations (2.2.11) and (2.2.12) can be used to compute the voltage waves $v_-(0,t)$ and $v_+(d,t)$. Now the new modal waveform can be found simply using the eigenvector matrices

$$\bar{u}_-(0,t) = P^{-1}\bar{v}_-(0,t),\tag{2.2.13}$$

$$\bar{u}_+(d,t) = P^{-1}\bar{v}_+(d,t).\tag{2.2.14}$$

Numerical procedures for analysis of transients in a network containing lossless transmission lines are described in the next chapter.

CHAPTER 3

NUMERICAL ALGORITHM

A computer program, called LSPICE, has been developed on the basis of the algorithm described in the previous chapter. This program can be used for simulating the DC analysis and the transient analysis of network containing coupled lossless transmission lines.

3.1. Modified Nodal Analysis of Lossless Transmission Lines

In this section, modified nodal analysis(MNA), used to form the lossless transmission lines equation modeling, is briefly introduced.

From Fig. 2.2.1 representing the equivalent circuit of an N-conductor lossless transmission line, we can define the modified nodal equation matrix for coupled lossless transmission lines shown in Fig. 3.1.1.

	$n1^m$	$n2^m$	$n3^m$	$n4^m$	$IBR1^m$	$IBR2^m$
$n1^m$					1	-1*
$n2^m$					-1*	1
$n3^m$					-1	
$n4^m$						-1
$IBR1^m$	1		-1			
$IBR2^m$		1		-1		

Fig. 3.1.1 Modified Nodal Equation Matrix for Coupled Lossless Transmission Lines - entries related to m^{th} Conductor

The superscript "m" denotes the m^{th} conductor in transmission line. $n1, n2, n3,$ and $n4$ are node numbers shown in Fig. 2.2.1. $IBR1$ and $IBR2$ are the equation numbers for the current through VCVS of equivalent circuit for transmission lines. Mark "*" denotes items used during DC analysis only.

The characteristic admittance matrix of N-coupled lossless transmission lines is

$$[Y_0] = \begin{bmatrix} Y_{11} & Y_{12} & Y_{13} & \cdot & \cdot & \cdot & Y_{1N} \\ Y_{21} & Y_{22} & Y_{23} & \cdot & \cdot & \cdot & Y_{2N} \\ Y_{31} & Y_{32} & Y_{33} & \cdot & \cdot & \cdot & Y_{3N} \\ \cdot & \cdot & \cdot & \cdot & \cdot & \cdot & \cdot \\ \cdot & \cdot & \cdot & \cdot & \cdot & \cdot & \cdot \\ \cdot & \cdot & \cdot & \cdot & \cdot & \cdot & \cdot \\ Y_{N1} & Y_{N2} & Y_{N3} & \cdot & \cdot & \cdot & Y_{NN} \end{bmatrix} \quad (3.1.1)$$

The modified nodal equation matrix for a characteristic admittance of N-coupled lossless transmission lines is

		$n3^1$	$n3^2$	$n3^3$...	$n3^N$
		$n4^1$	$n4^2$	$n4^3$...	$n4^N$
$n3^1$	$n4^1$	Y_{11}	Y_{12}	Y_{13}	...	Y_{1N}
$n3^2$	$n4^2$	Y_{21}	Y_{22}	Y_{23}	...	Y_{2N}
$n3^3$	$n4^3$	Y_{31}	Y_{32}	Y_{33}	...	Y_{3N}
:	:	:	:	:	...	:
$n3^N$	$n4^N$	Y_{N1}	Y_{N2}	Y_{N3}	...	Y_{NN}

Fig. 3.1.2 Modified Nodal Equation Matrix for Characteristic Admittance Matrix

The modified nodal equation matrix for characteristic admittance matrix has the same form for the near end and far end equivalent circuits of transmission lines.

3.2. DC Analysis

The circuit equations are, in general, a system of algebraic-differential equations of the form

$$F(x, \dot{x}, t) = 0 \quad (3.2.1)$$

where x is the vector of unknown circuit variables, \dot{x} is the time derivative of x , and F is, in general, a nonlinear operator.

Circuit analysis determines the solution of (3.2.1) for different special cases that are of interest in the design of an electronic circuit. A DC analysis, for example, usually is invoked to determine the equilibrium solution of (3.2.1). In this case, the vector \dot{x} is zero, and (3.2.1) is simplified to a system of nonlinear equations.

For DC analysis of a network with a transmission line, we assume that the currents at the near end and far end nodes of transmission lines are identical. DC solution of a network with a transmission line can be calculated simply by setting -1 in terms $(n1, IBR2), (n2, IBR1)$ in the modified nodal equation matrix (in Fig. 3.1.1) and solving the reduced network equation. The result of this procedure is the DC solution of a network without a transmission line. It is based on the observation that at steady state, the two ends of each conductor of a lossless transmission line are at the same voltage.

3.3. Tracking of Wave Propagation

To evaluate the voltage sources of the equivalent circuit we must know the magnitudes of the conductor voltages of the incoming waves at the ends of the transmission line. At the initial time instant, we can either set the magnitudes of those voltage sources to zero, if line was originally uncharged, or calculate their initial steady-state values from DC analysis, and then solve the augmented network. Once the augmented network is solved, the magnitudes of voltage waves leaving the ends of each transmission line can be calculated. Tracking the wave propagation, we can obtain the magnitudes of the conductor voltages of the incoming waves at the ends of each transmission line at the next time step. Thus the transient behavior of the network can be calculated. Since we only know the propagation delay times of the modes, we have to decompose the waves into their modal components in order to track their propagation. We then have to recombine those modal components to obtain the magnitudes of the total voltage waves.

The magnitudes of the voltage sources, \bar{e}_L and \bar{e}_R are related to the modal waveforms, \bar{u}_- and \bar{u}_+ , by

$$\bar{e}_L(t) = 2P\bar{u}_-(0, t), \quad (3.3.1)$$

$$\bar{e}_R(t) = 2P\bar{u}_+(d, t), \quad (3.3.2)$$

where

$$\bar{e}_L(t) = [e_{L1}(t), \dots, e_{Lm}(t), \dots, e_{LN}(t)]^T, \quad (3.3.3)$$

$$\bar{e}_R(t) = [e_{R1}(t), \dots, e_{Rm}(t), \dots, e_{RN}(t)]^T, \quad (3.3.4)$$

$$\bar{u}_+(d, t) = [u_+^1(d, t), \dots, u_+^m(d, t), \dots, u_+^N(d, t)]^T, \quad (3.3.5)$$

$$\bar{u}_-(0, t) = [u_-^1(0, t), \dots, u_-^m(0, t), \dots, u_-^N(0, t)]^T. \quad (3.3.6)$$

and where the superscript m denotes the m^{th} modal component, and the letter d represents the line length.

We define a time delay operator $D(\Delta t)$ such that

$$D(\Delta t)f(x, t) = f(x, t - \Delta t). \quad (3.3.7)$$

$D(\Delta t)$ behaves like a delay line. It delays the appearance of a signal by a time duration of Δt .

We know that $u_-(x, t)$ represents the backward traveling modal waveform, and $u_+(x, t)$ represents the forward traveling modal waveform of a transmission line. We also know that

$$\begin{aligned} \bar{u}_-(0, t) &= \bar{u}_-(t - \tau d + \tau d) \\ &= \bar{u}_-(d, t - \tau d) \\ &= D(\tau d)\bar{u}_-(d, t) \\ &= D(\tau d)[P^{-1}\bar{v}_-(d, t)], \end{aligned} \quad (3.3.8)$$

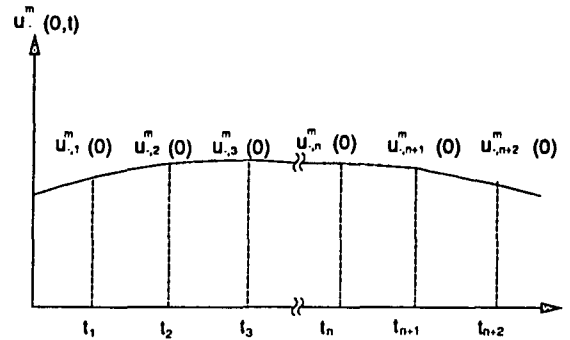
where $D(\tau d)$ is a diagonal matrix containing modal time delays. Analogously we write

$$\begin{aligned} \bar{u}_+(d, t) &= \bar{u}_+(t - \tau d) \\ &= \bar{u}_+(0, t - \tau d) \\ &= D(\tau d)\bar{u}_+(0, t) \\ &= D(\tau d)[P^{-1}\bar{v}_+(0, t)], \end{aligned} \quad (3.3.9)$$

where again $D(\tau d)$ is an $N \times N$ diagonal matrix of modal time delays.

The relations (3.3.8) and (3.3.9) are based on the fact that an i^{th} component of modal waveform takes a time of $\tau_i d$ to travel the length of the transmission line. Thus once we know the time when a component of modal waveform leaves one end of the transmission line, we can compute the time at which it arrives at the other end. However, since there can be more than one multiconductor transmission line system in a network, an efficient method of tracking the wave propagation is necessary. This algorithm is briefly described below.

a)



b)

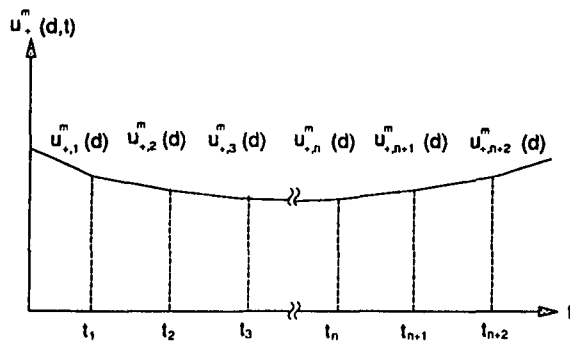


Fig. 3.3.1 Discretization of Modal Wave;
 a) Left Traveling Wave at the Left Boundary ($x=0$)
 b) Right Traveling Wave at the Right Boundary ($x=d$)

The quantities $u_m^m(0, t)$ and $u_m^m(d, t)$ are discretized, as shown in Fig. 3.3.1 for the purpose of tracking the wave propagation (Liao, 1989). It should be noted here that the time intervals between the discrete moments t_k are not necessarily the same as those determined by the steps in the numerical integration.

We now introduce the notation

$$u_{-,n}^m(0) = u_-^m(0, t_n), \quad (3.3.10)$$

and use (3.3.8) to write

$$u_{-,n}^m(0) = u_-^m(d, t_n - \tau d). \quad (3.3.11)$$

Analogously introducing the notation

$$u_{+,n}^m(d) = u_+^m(d, t_n), \quad (3.3.12)$$

and using (3.3.9) we can write

$$u_{+,n}^m(d) = u_+^m(0, t_n - \tau d). \quad (3.3.13)$$

The values of the modal waveforms $u_{-,k}^m(0)$, $u_{+,k}^m(d)$, and t_k are stored in memory at each time point. At time t , of the numerical integration, we can find time factors for modal wave tracking before the delay time such that

$$t_n \leq t - t_d \leq t_{n+2}$$

$$p_1(t) = \frac{\{(t - t_d) - t_{n+1}\} \{(t - t_d) - t_{n+2}\}}{(t_n - t_{n+1})(t_n - t_{n+2})}, \quad (3.3.14)$$

$$p_2(t) = \frac{\{(t - t_d) - t_n\} \{(t - t_d) - t_{n+2}\}}{(t_{n+1} - t_n)(t_{n+1} - t_{n+2})}, \quad (3.3.15)$$

$$p_3(t) = \frac{\{(t - t_d) - t_n\} \{(t - t_d) - t_{n+1}\}}{(t_{n+2} - t_n)(t_{n+2} - t_{n+1})}. \quad (3.3.16)$$

We then obtain $u_-^m(0, t)$ and $u_+^m(d, t)$ by interpolation as follows:

$$u_-^m(0, t) = u_-^m(0, t_n)p_1(t) + u_-^m(0, t_{n+1})p_2(t) + u_-^m(0, t_{n+2})p_3(t), \quad (3.3.17)$$

$$u_+^m(d, t) = u_+^m(d, t_n)p_1(t) + u_+^m(d, t_{n+1})p_2(t) + u_+^m(d, t_{n+2})p_3(t). \quad (3.3.18)$$

Let us observe for example a modal wave tracking at the time t using the described algorithm. We need to find a m^{th} modal waveform at the time $t-t_d$ before the delay time. If the time $t-t_d$ equals to t_{n+1} , the time factors, $p_1(t)$ and $p_3(t)$ in equation, (3.3.14), (3.3.16) are zero and $p_2(t)$ in equation (3.3.15) is 1. From those time factor values, the m^{th} modal wave voltages at the time t can be found from equations, (3.3.17),(3.3.18) as follows

$$u_-^m(0, t) = u_-^m(0, t_{n+1}), \quad (3.3.19)$$

$$u_+^m(d, t) = u_+^m(d, t_{n+1}). \quad (3.3.20)$$

Using equations, (3.3.19),(3.3.20), the modal waveforms at the time t can be found. It is very important to obtain the accurate solutions of simulation of networks with coupled transmission lines.

3.4. Procedure for the Transient Analysis

For analysis in time domain, an equivalent network consisting of lumped elements can be derived to replace the coupled lines. Let us observe for example a coupled line system at the near end ($x = 0$). Since the line voltage is the sum of the incoming voltage wave \bar{v}_- and the outgoing voltage wave \bar{v}_+ , while the line current is a difference between the two current waves, \bar{i}_+ and \bar{i}_- ,

$$\bar{v}(0, t) = \bar{v}_+(0, t) + \bar{v}_-(0, t), \quad (3.4.1)$$

$$\bar{i}(0, t) = \bar{i}_+(0, t) - \bar{i}_-(0, t). \quad (3.4.2)$$

Substitution of equations (2.2.1), (2.2.3) at $x = 0$ into (3.4.1) yields

$$\bar{v}(0, t) = Y^{-1}\bar{i}(0, t) + 2\bar{v}_-(0, t). \quad (3.4.3)$$

The equivalent circuit is based on equation (3.4.3). We note in (3.4.3) that the term $2\bar{v}_-(0, t)$ denotes the voltage wave that starts at the far end, $x=d$, and reaches the near end. The voltage wave that enters the far end can be derived from (2.2.2),(2.2.4),(2.2.8) at $x=d$ to obtain

$$2\bar{v}_+(d, t) = \bar{v}(d, t) - Y^{-1}\bar{i}(d, t). \quad (3.4.4)$$

Since there are different delays due to different speeds of propagation, we need to decompose the voltage given by (3.4.4) into its modal components. This is achieved by using (2.2.3), (2.2.4) like as (2.2.11),(2.2.12) to multiply the right-hand side of (3.4.4) by the inverse eigenvector matrix, P^{-1} . Each element of the resultant vector, which collectively represents the magnitudes for each different speed, is then delayed by appropriate delay times. On reaching the near end, the resultant voltages are then obtained by combining all the components according to the transformation matrix P . We therefore have

$$2\bar{v}_-(0, t) = P \{P^{-1}[\bar{v}(d, t) - Y^{-1}\bar{i}(d, t)]\}D(\tau d), \quad (3.4.5)$$

where $D(\tau d)$ is used as a diagonal matrix of time delay operators.

Upon substituting (3.4.5) into (3.4.3), there results

$$\bar{v}(0, t) = Y^{-1}\bar{i}(0, t) + P \{P^{-1}[\bar{v}(d, t) - Y^{-1}\bar{i}(d, t)]\}D(\tau d). \quad (3.4.6)$$

Similarly, we have

$$\bar{v}(d, t) = Y^{-1}\bar{i}(d, t) + P \{P^{-1}[\bar{v}(0, t) - Y^{-1}\bar{i}(0, t)]\}D(\tau d). \quad (3.4.7)$$

Equations (3.4.6) and (3.4.7) can be considered as the branch constitutive relations for the voltage sources shown in Fig. 2.2.1. These two equations can be programmed straightforwardly to simulate coupled line systems in the time domain. Since the difference

between the two current waves, \bar{i}_+ and \bar{i}_- at the time $t = 0$ is zero, the line current, $\bar{i}(x, t)$ is zero. Therefore, from equations, (3.4.3), (3.4.4), we can find the initial voltage waves at $x = 0$ and $x = d$ as follows:

$$\bar{v}_-(0, 0) = \frac{\bar{v}(0, 0)}{2}, \quad (3.4.8)$$

$$\bar{v}_+(d, 0) = \frac{\bar{v}(d, 0)}{2}. \quad (3.4.9)$$

These equations (3.4.8),(3.4.9) are used for setting the initial modal waveforms at the each end for the transient analysis of a network with coupled lossless transmission lines.

The procedure for transient analysis of a network containing coupled lossless transmission lines in LSPICE can be summarized as follows

1. Replace the composite circuit elements with their equivalent circuits.
2. Form the system matrix using modified nodal analysis.
3. Perform DC analysis of the network (at initial instant of time)
4. Set the initial modal waveforms as (3.4.8),(3.4.9).
5. Calculate the amplitudes of the left and right traveling modal waves using (3.4.4),(3.4.5),(3.4.6), and (3.4.7).
6. Advance the time step.
7. Determine the amplitude of the incoming waves at both ends of each transmission line using the technique of modal wave tracking.
Calculate the amplitude of the corresponding equivalent voltage

sources using (2.2.3),(2.2.4).

8. Solve the network.

9. Repeat steps 5,6,7, and 8 until the transient analysis is completed.

CHAPTER 4

COMPUTER IMPLEMENTATION IN SPICE

In this chapter a description of computer implementation of multiconductor coupled transmission line modes in SPICE is given. Other elements such as passive R,L,C components and transistors are modelled as described in the "Program reference for SPICE2" (Cohen, 1976). The subjects to be discussed in this section include the input format, linked list specifications, element load structure.

4.1. Input Format

The specification of network and its components is contained in an input file which like in the case of SPICE is in free format. Fields on a card (command and statement) are separated by one or more blanks, a comma, an equal (=) sign, or a left or right parenthesis; extra spaces are ignored. A card may be continued by a + (plus) in column 1 of the following card; SPICE continues reading beginning with column 2. A name field must begin with a letter (A through Z) and cannot contain any delimiters. Only the first eight characters of the name are used. A name field of a coupled lossless transmission line begin with a letter Y. The number of conductors in one transmission line system is limited to 20 and the number of transmission line systems is limited to 10. These are practical programming restrictions and can be changed if necessary.

The general form of a statement defining a conductor in coupled lossless

transmission line is as follows:

```
YXXXXXXX N1 N2 T=INTEGER N=INTEGER D=VALUE C1=VALUE
<C2=VALUE ...> L1=VALUE <L2=VALUE ...>
```

N1 is the node at near end; N2 is the node at far end. T is the identifier of transmission line system; N is the conductor number in the transmission line system; D is the length of transmission line; The length is specified once per system; C1,C2,... are the distributed capacitances (strictly speaking they are coefficients of electrostatic inductance) of transmission line; L1,L2,... are the distributed inductances of transmission line. The usage of unit of length in D,L, and C must be consistent.

An example of specification for a coupled transmission line system with two conductors shown in Fig. 5.1.1 is given below

```
Y1 2 3 T=1 N=1 D=300 C1=0.1P C2=-0.04P L1=500P L2=300P
Y2 4 5 T=1 N=2 C1=-0.04P C2=0.1P L1=300P L2=500P
```

It should be pointed here that LSPICE will always use a transient time step which does not exceed one half of the minimum transmission line delay. Consequently the presence of short transmission lines with propagation delay which is short in comparison with the overall analysis timeframe will cause long run times (Cohen, 1976).

4.2. Block Diagram of LSPICE

The block diagram of LSPICE is shown in Fig. 4.2.1.

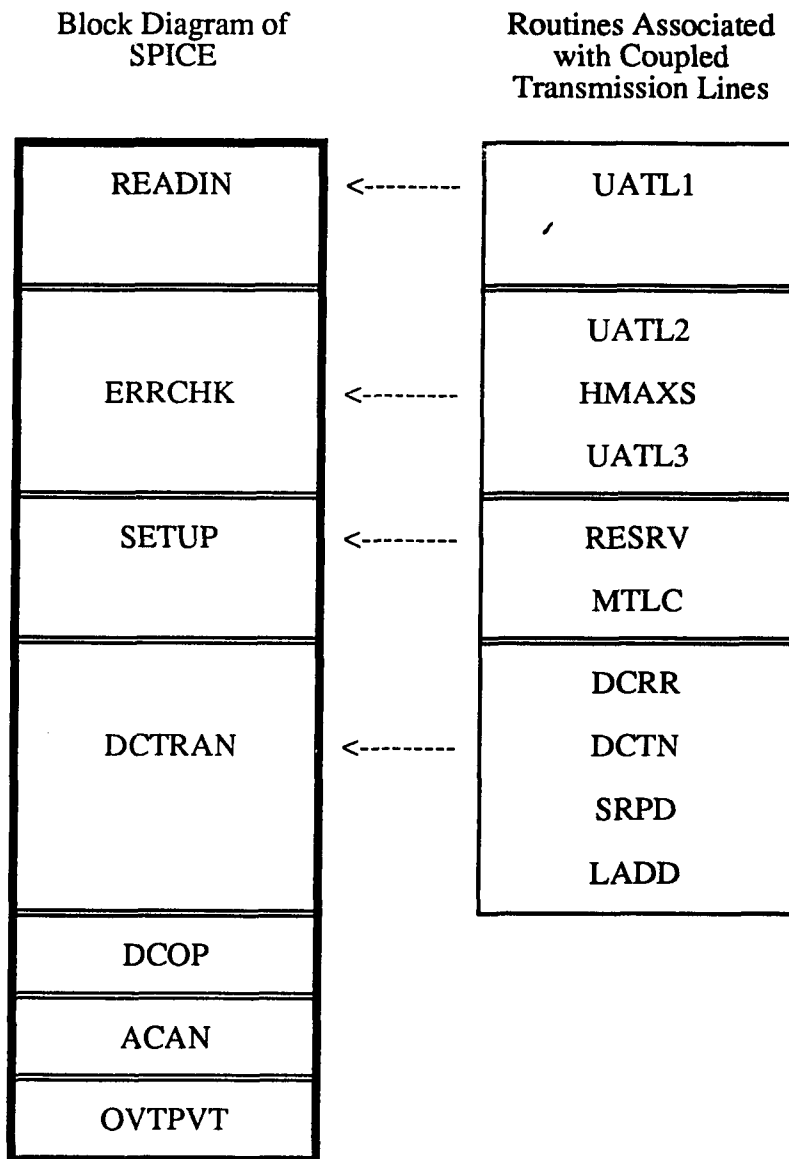


Fig. 4.2.1 Block Diagram of LSPICE

The routine UATL1 is called from READIN in SPICE to read the input files. This routine reads the input file searches for specification of coupled lossless transmission lines, and creates the transmission line data structure. The routines UATL2, UATL3, and HMAXS are called from ERRCHK in SPICE to check the circuit description for common user errors, and calculate the information pertaining to coupled transmission line system (eigenvector, delay time, characteristic impedance, etc.). In addition, UATL3 also prints the transmission model parameter listing. Once READIN and ERRCHK are executed, the preparation for circuit analysis can begin. The routines RESRV and MTLC are called from SETUP to construct the integer pointer structure used by DCTRAN. The RESRV establishes the integer pointer structure of nonzero Y-matrix terms. The MTLC subroutine computes and stores the pointer locations that are used to construct the Y matrix. After SETUP has executed successfully, the circuit analysis can proceed. The routines DCRR, DCTN, SRPD, and LADD are called from DCTRAN to determine the transient initial conditions, and the transient analysis. The routines DCRR, DCTN, and SRPD compute and store the equivalent voltage sources $e_L(t)$, $e_R(t)$ and the modal waveforms, $u_-^m(0, t)$, $u_+^m(d, t)$ for coupled transmission line. The routine LADD constructs the nodal equation for specific iteration.

4.3. Linked List Specification

After reading the input data, LSPICE builds a list of vectors that contain the basic information about all the elements, the required analysis and output requests. The vector LOCATE(50) contains the pointers to each list head element; element types are referenced

through the ID identifier. Inside this vector all integer data are referenced using the LOC pointer, while all real data are accessed using the LOCV pointer.

Each list element generally contains both integer and real data. Even though both data types require only one word of memory on the computer, separate subscripts are used to access the two types. All integer data is referenced using the array NODPLC; all real (and character) data is accessed using the equivalenced array VALUE. The VALUE-subscript for the first real value is stored in the integer part of the list element and is called LOCV (LOCM for device models); the NODPLC subscript is called LOC. In the detailed list-element structure to follow, notation is defined only on first use (Cohen, 1976).

Linked list specifications for coupled lossless transmission line is as following:

ID=16		
LOC+ 0: next-pointer	LOCV+ 0: element name	
+ 1: LOCV	+ 1: T.L. length	
+ 2: n1 (near end)	+ 2: delay time	
+ 3: n2 (far end)	+ 3: unused	
+ 4: n5 (ground)	+ 4: unused	
+ 5: system ID (=JID)	+ 5: velocity	
+ 6: n3 (=ND1(JID(IND)))	+ 6: C1	+26: L1
+ 7: n4 (=ND2(JID(IND)))	+ 7: C2	+27: L2
+ 8: IBR1	+ 8: C3	+28: L3
+ 9: IBR2	+ 9: C4	+29: L4
+10: line ID (=IND)	+10: C5	+30: L5
+11: (IBR1,n1)	+11: C6	+31: L6
+12: (n1,IBR1)	+12: C7	+32: L7
+13: (IBR1,n3)	+13: C8	+33: L8
+14: (n3,IBR1)	+14: C9	+34: L9
+15: (IBR2,n2)	+15: C10	+35: L10
+16: (n2,IBR2)	+16: C11	+36: L11
+17: (IBR2,n4)	+17: C12	+37: L12
+18: (n4,IBR2)	+18: C13	+38: L13
+19: (IBR1,n2)	+19: C14	+39: L14
+20: (IBR2,n1)	+20: C15	+40: L15
+21: LTD offset	+21: C16	+41: L16

```

do 10 L=1,inl(JID)          +22: C17   +42: L17
+23+m: (n3,ND1(JID,L))    +23: C18   +43: L18
+24+m: (n4,ND2(JID,L))    +24: C19   +44: L19
      m=m+2                +25: C20   +45: L20
10 continue

```

LTD +0: past value (incident modal wave)
+1: past value (reflected modal wave)

The "next-pointer" points to the next element of the same ID. If there is no next element, "next-pointer" is zero. "LOCV" points to the real-valued storage for the element. The symbols n1 and n2 are near end and far end node numbers, respectively. During READIN, these are the node numbers read from input. The symbols n3 and n4 are additional node numbers for those nodes added to accommodate equivalent circuit of transmission line. After ERRCHK, this entry is replaced by an index into the JUNODE array for the compact renumbered node list. "IBR" is the equation number for the current flowing in this element. "JID" and "IND" are transmission line system and conductor identification integer numbers, respectively. The notation "(a,b)" means a pointer to matrix location (a,b): the a'th row, b'th column entry. "element name" is the element name, left-justified, with blank fill to 8 characters. "T.L. length" is the length of the transmission line. "delay time" and "velocity" are the delay time and the velocity of transmission line computed in subroutines UATL2,HMAXS, respectively. "C1,...,C20" and "L1,...,L20" are the elements of capacitance and inductance matrices of transmission lines. "LTD offset" is the offset this element into any of the LTD table in the memory which is used during analysis to store the modal waveform at the previous time point for modal wave tracking. "inl(JID)" indicates the number of line where the transmission line system ID is JID.

4.4. Element Load Structure

This section describes the various element "stamps" or locations in the circuit equation coefficient matrix to which different elements add. The subroutine LADD was constructed as a following element load structure for coupled transmission lines. This structure was given using modified modal equation matrix for coupled transmission lines described in section 3.1. The notation for coupled lossless transmission lines used below is described in the following figure:

```

A(i(v1),n1) = +1
A(n1,i(v1)) = +1
A(i(v1),n3) = -1
A(n3,i(v1)) = -1
A(i(v2),n2) = +1
A(n2,i(v2)) = +1
A(i(v2),n4) = -1
A(n4,i(v2)) = -1
A(i(v1),n2) = -1*
A(i(v2),n1) = -1*
B(i(v1)) = vrefg(jid,ind)*2.0
B(i(v2)) = vincl(jid,ind)*2.0
do 10 L=1,INL(JID)
A(n3,nd1(jid,L)) = Y0(jid,ind,L)
A(n4,nd2(jid,L)) = Y0(jid,ind,L)
10 continue

```

The symbols n1,n2,n3, and n4 are the element nodes. i(v1) and i(v2) are the equation added to the modified nodal equations to solve for the current in elements v1,v2. A() B() are the modified nodal coefficient matrix and the right-hand side for the set of circuit equations, respectively. "vrefg" and "vincl" are backward and forward modal wave voltages at the near end and the far end for specific iteration, respectively. Mark "*" denotes items,

$A(i(v1),n2)$, $A(i(v2),n1)$, used during DC analysis only. This structure uses the subroutine LADD for coupled transmission lines during all of the analysis procedures. The subroutine LOAD constructs the linearized system of nodal equations for specific iterate.

4.5. Application of Input Processing Module

In this section, example of input processing for interconnection equation modules of circuit is shown. A program for processing of input files describing circuit and interconnections, called SIP, has been developed during the course of this work. This program can be used as a library function or a tool for an input processing. An example of network with transmission line is given. After READIN and ERRCHK for circuit, a unified internal representation is constructed.

Example of processing of specification of a coupled lossless transmission line as following:

```

write COMMON statements
...
CALL SIP
...
IF (JELCNT(16).EQ.0) GO TO NEXT ROUTINE
LOC=LOCATE(16)
FIRST
IF (LOC.EQ.0) GO TO NEXT ROUTINE
LOCV=NODPLC(LOC)
NODE1=NODPLC(LOC+2)
NODE2=NODPLC(LOC+3)
GROUND NODE=NODPLC(LOC+4)
T.L. SYSTEM I.D.(=jid)=NODPLC(LOC+5)
NODE3=NODPLC(LOC+6)
NODE4=NODPLC(LOC+7)
LINE I.D.(=ind)=NODPLC(LOC+10)
ELEMENT NAME=VALUE(LOCV)
T.L. LENGTH=VALUE(LOCV+1)

```

```

DELAY TIME=VALUE(LOCV+2)
VELOCITY=VALUE(LOCV+5)
C(jid,ind,1)=VALUE(LOCV+6)
C(jid,ind,2)=VALUE(LOCV+7)
.
.
.
C(jid,ind,20)=VALUE(LOCV+25)
L(jid,ind,1)=VALUE(LOCV+26)
L(jid,ind,2)=VALUE(LOCV+27)
.
.
.
L(jid,ind,20)=VALUE(LOCV+45)
LOC=NODPLC(LOC)
GO TO FIRST
NEXT ROUTINE

```

"COMMON" statement defines one or more contiguous areas or blocks of storage. Also, "COMMON" statements define the order in which variables and arrays are stored in each common block. The COMMON statements for circuit input processing and interconnection equation modules are shown in APPENDIX B. Identification number for coupled transmission lines defines 16. So, the JELCNT(16) stores the total number of coupled transmission lines and the LOCATE(16) contains the pointer to the first element with a coupled transmission line. Inside this vector all integer data and real data structures are given using linked list specifications described in Section 4.3.

4.6. Application of Interconnection Equation Module

The equation matrix is very sparse - typically, over 85 % of its entries are zeros (Nagal, 1975). The matrix structure is stored internally during the setup process. Initially,

the nonzero matrix entries are recorded using a set of link lists, one for each row of the matrix. The actual matrix entries are stored in table LVN in parallel. The offsets within the LVN table to each matrix term which a given circuit element increments are stored with each circuit element. In this way, the overhead mapping of an (i,j) matrix location to its proper offset within the LVN table occurs only once. For example, a resistor between nodes N1 and N2 causes an addition or subtraction to matrix terms (N1,N1), (N1,N2), (N2,N1), and (N2,N2). The locations of each of these terms is stored together with a value of each resistor. As the result, this LVN table contains the system of circuit equations, the equation coefficients and the right-hand side vector.

All of the analysis procedures use the subroutine LOAD. The subroutine LOAD constructs the linearized system of nodal equations for specific iterate. The contributions to the Y-matrix from nonlinear devices are computed separately in the subroutines DIOD, BJT, JEFT, and MOSFET.

An example of application to interconnection equation module is as following:

```

write COMMON statement
...
CALL SIP
...
CALL LOAD
...
if want to print out MNA matrix
CALL MNAM
...
CALL SIZMEM(IRPT,IRPTS)
DO 10 I=1,IRPTS
IF (I .GT. NSTOP) GO TO 5
B(I)=VALUE(LVN+I)
GO TO 10
5  IR=NODPLC(IROWNO+I)
   IC=NODPLC(JCOLNO+I)
   A(IR,IC)=VALUE(LVN+I)
10 CONTINUE

```

```
...  
write solving program  
...  
exit
```

The modified nodal equation matrix for a circuit can be shown by calling subroutine MNAM. The subroutine SIZMEM sets IRPTS to the size of the table pointed to by table pointer IRPT. This helps to find the number of nonzero entries. NSTOP indicates the number of circuit equations. IROWNO and JCOLNO mean a table pointer to a table containing the row number and column number for the nonzero entries, respectively. A(i,j) and B(i) are the modified nodal coefficient matrices (NSTOP x NSTOP) and the right-hand side vector (NSTOP x 1) for the set of circuit equations.

CHAPTER 5

NUMERICAL EXPERIMENTS

The transient responses of four networks were simulated using LSPICE and UANTL programs. The results obtained in the simulation of those four examples are summarized and discussed here. The first example is a linear network containing two-conductor lossless transmission lines. The second one is a linear network containing two three-conductor lossless transmission lines. The third example is a nonlinear network containing one two-conductor transmission line. The final example is a nonlinear network containing two transmission line systems one with two-conductors and another one with three-conductors. The examples selected here are those studied in [Liao, 1989; Palusinski, et al., 1990] and simulated using UANTL. This gives good basis for comparison and verification of performance of LSPICE, especially for systems with nonlinear terminations which cannot be solved by exact analytical means.

5.1. Simulation of a Linear Network Containing One Transmission Line System

A simple example of linear network containing a coupled, two conductor lossless transmission line is shown in Fig. 5.1.1.

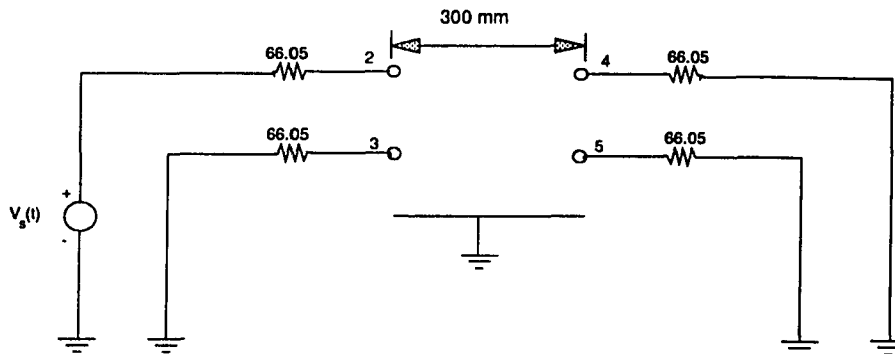


Fig. 5.1.1 A Linear Network containing a Two-Conductor Transmission Line System.

The $[L]$ and $[C]$ matrices of the transmission line system are

$$[L] = \begin{bmatrix} 500 & 300 \\ 300 & 500 \end{bmatrix}$$

$$[C] = \begin{bmatrix} 0.10 & -0.04 \\ -0.04 & 0.10 \end{bmatrix}$$

The units of $[L]$ and $[C]$ are $\frac{\mu H}{mm}$ and $\frac{pF}{mm}$, respectively and the length of coupled lines is $D=300$ mm. The first line is driven by a voltage source with impedance equal to the line matched-load impedance, and the time-dependent voltage is shown in Fig. 5.1.2.

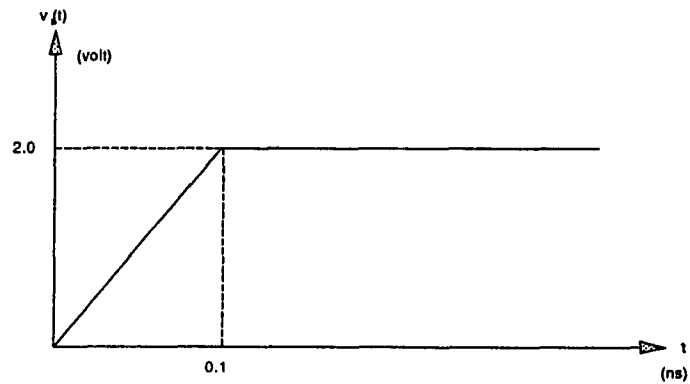


Fig. 5.1.2 Driving Voltage of the Network in Fig. 5.1.1.

The transient in the network was calculated using an analytical method and simulated using LSPICE and UANTL for a time interval of 9.0 nsec. The solutions obtained in the three cases were compared. The transient response was simulated with the tolerance parameter for local truncation error set to 10^{-4} . Voltages at node 2, node 3, node 4, and node 5, were plotted and are shown in Fig. 5.1.3, Fig. 5.1.4.

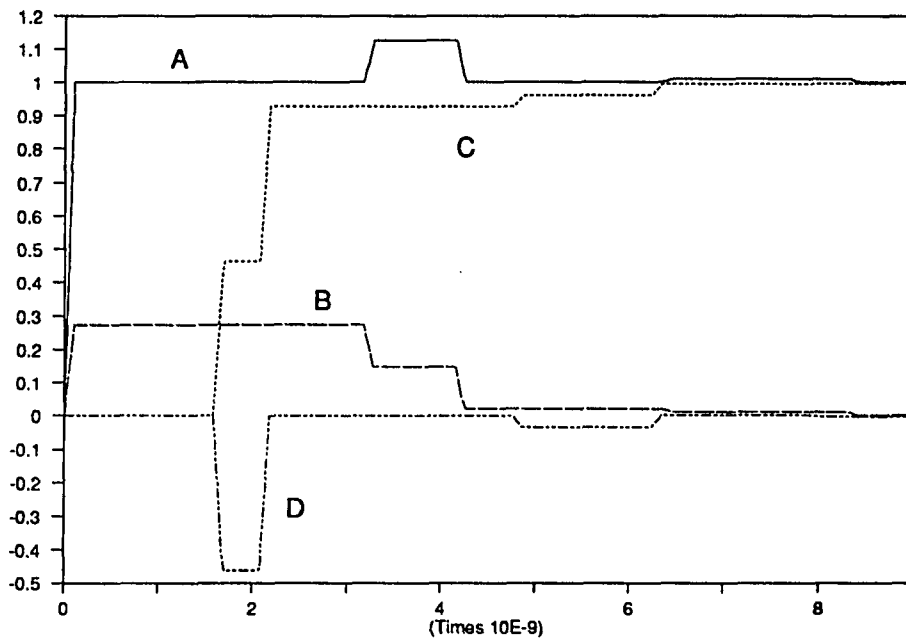


Fig. 5.1.3 Transient Response calculated by LSPICE with $RELTOL=10^{-4}$;
A: Voltage at node 2; B: Voltage at node 3;
C: Voltage at node 4; D: Voltage at node 5.

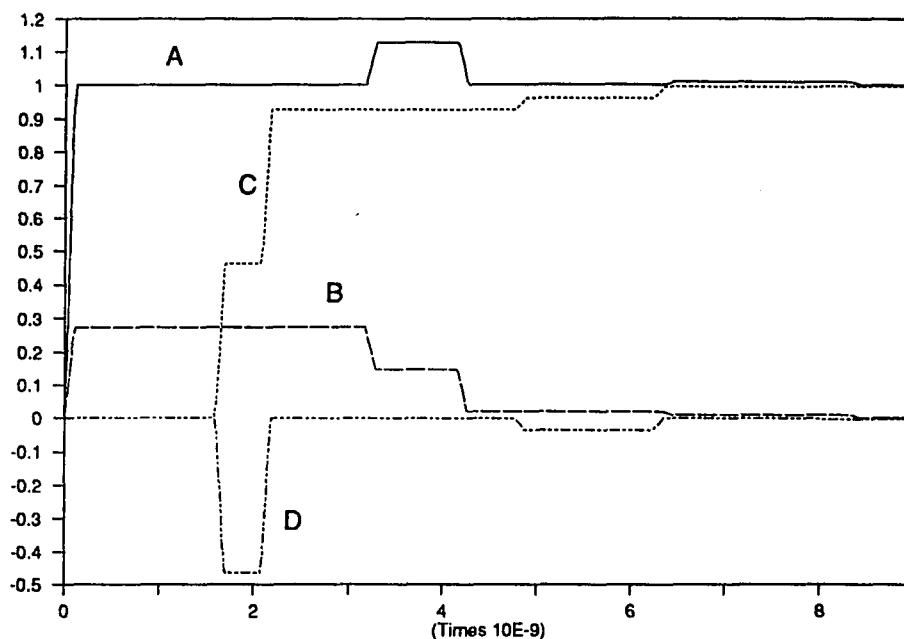


Fig. 5.1.4 Transient Response calculated by UANTL with $ETOL=10^{-4}$;
 A: Voltage at node 2; B: Voltage at node 3;
 C: Voltage at node 4; D: Voltage at node 5.

The CPU time required for the simulation with same local truncation error settings are as follows

LSPICE ($RELTOL=10^{-4}$) = 34 sec

UANTL ($ETOL=10^{-4}$) = 23 sec

For the purpose of comparison, the voltages at node 4 and node 5 were computed using an analytical method. The delay time of the first line and the second line are 1.5875

nsec and 2.0785 nsec, respectively. The percentage errors between analytical results and LSPICE and UANTL are calculated at a number of time points. The results are shown in Table 5.1.1 and Table 5.1.2.

Table 5.1.1 Percentage Error in Voltages at Node 4
from the Reference Value

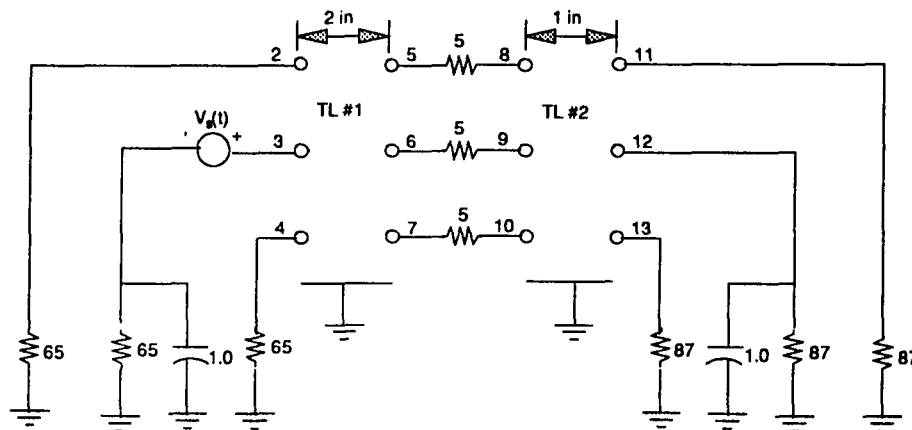
Time	Analytic	LSPICE		UANTL	
		RELTOL=10 ⁻⁴		ETOL=10 ⁻⁴	
(ns)	(volt)	(volt)	% error	(volt)	% error
1.000	0.00000	0.00000	0.0	0.00000	0.0
1.553	0.00000	0.00000	0.0	0.00001	0.0
1.575	0.00000	0.00000	0.0	0.00004	0.0
1.590	0.01181	0.01180	0.1	0.02961	151.0
2.000	0.46300	0.46300	0.0	0.46300	0.0
3.000	0.92600	0.92590	0.0	0.92590	0.0
4.000	0.92600	0.92590	0.0	0.92590	0.0
5.000	0.96031	0.96020	0.0	0.96020	0.0
6.000	0.96031	0.96020	0.0	0.96020	0.0
7.000	0.99466	0.99450	0.0	0.99450	0.0
8.000	0.99634	0.99610	0.0	0.99600	0.0
9.000	0.99725	0.99710	0.0	0.99700	0.0

Table 5.1.2 Percentage Error in Voltages at Node 5
from the Reference Value

Times (ns)	Analytic (volt)	LSPICE RELTOL=10 ⁻⁴		UANTL ETOL=10 ⁻⁴	
		(volt)	% error	(volt)	% error
1.000	0.00000	0.00000	0.0	0.00000	0.0
1.553	0.00000	0.00000	0.0	-0.00001	0.0
1.575	0.00000	0.00000	0.0	-0.00001	0.0
1.590	-0.01181	-0.01180	0.1	-0.02961	151.0
2.000	-0.46300	-0.46300	0.0	-0.46300	0.0
3.000	0.00000	-0.00005	0.0	-0.00005	0.0
4.000	0.00000	-0.00005	0.0	-0.00005	0.0
5.000	-0.03431	-0.03432	0.0	-0.03432	0.0
6.000	-0.03431	-0.03432	0.0	-0.03430	0.0
7.000	0.00000	0.00000	0.0	0.00000	0.0
8.000	-0.00164	-0.00160	2.4	-0.00159	3.1
9.000	-0.00259	-0.00254	1.9	-0.00254	1.9

It can be observed that the modal waveform obtained using UANTL reached the far end of transmission line before delay time (1.5875 nsec) of the first line. This points to an inaccuracy in wave tracking algorithm. The percentage error at the time point 1.59 ns is 151 % (0.018 V). The errors observed here are not excessive, but they may be magnified in case of strong reflections. The results obtained using LSPICE agree with the ones obtained using the analytical method. From these results, we conclude that the modal wave tracking algorithm implemented in LSPICE is more accurate than that of UANTL. The UANTL requires less CPU time for simulation of this specific example.

5.2. Simulation of a Linear Network Containing Two Transmission Line Systems



unit: R: Ohm; C: pF

Fig. 5.2.1 A Linear Network containing Two Transmission Line Systems

A network composed of three simple linear subnetworks interconnected by two transmission lines is shown in Fig. 5.2.1.

The [L] and [C] matrices of transmission line # 1 are

$$[L] = \begin{bmatrix} 3.792 & 0.836 & 0.292 \\ 0.836 & 3.753 & 0.836 \\ 0.292 & 0.836 & 3.792 \end{bmatrix}$$

$$[C] = \begin{bmatrix} 0.883 & -0.102 & -0.0779 \\ -0.102 & 0.899 & -0.102 \\ -0.0779 & -0.102 & 0.883 \end{bmatrix}$$

The [L] and [C] matrices of transmission lines # 2 are

$$[L] = \begin{bmatrix} 5.033 & 1.734 & 0.818 \\ 1.734 & 4.792 & 1.734 \\ 0.818 & 1.734 & 5.033 \end{bmatrix}$$

$$[C] = \begin{bmatrix} 0.677 & -0.163 & -0.0145 \\ -0.163 & 0.722 & -0.163 \\ -0.0145 & -0.163 & 0.677 \end{bmatrix}$$

The units of [L] and [C] in both cases are $\frac{nH}{cm}$ and $\frac{pF}{cm}$, respectively.

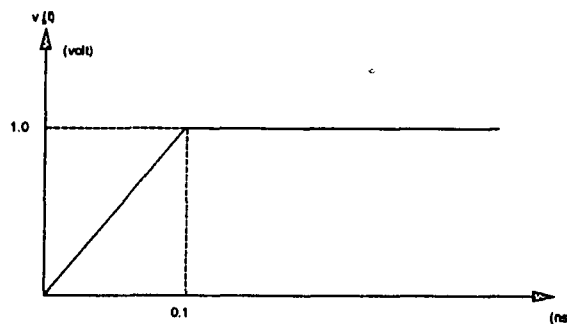


Fig. 5.2.2 Driving Voltage of the Network in Fig. 5.2.1.

The lines were initially uncharged and the transients were caused by the voltage source, $V_s(t)$, rising from zero to 1 volt in 100 ps. The network was simulated using LSPICE and UANTL for time interval of 3.0 ns. The transient responses were simulated with local truncation error set to 10^{-3} , and 10^{-4} , respectively. Voltages at node 2, node 3, node 11, and node 12 were plotted and are shown in Fig. 5.2.3 and Fig. 5.2.4 for LSPICE and UANTL, respectively. The voltages at node 2 and node 11 have a much smaller magnitude than those on node 3 and node 12, and thus they are shown separately in Fig. 5.2.5 and Fig. 5.2.6.

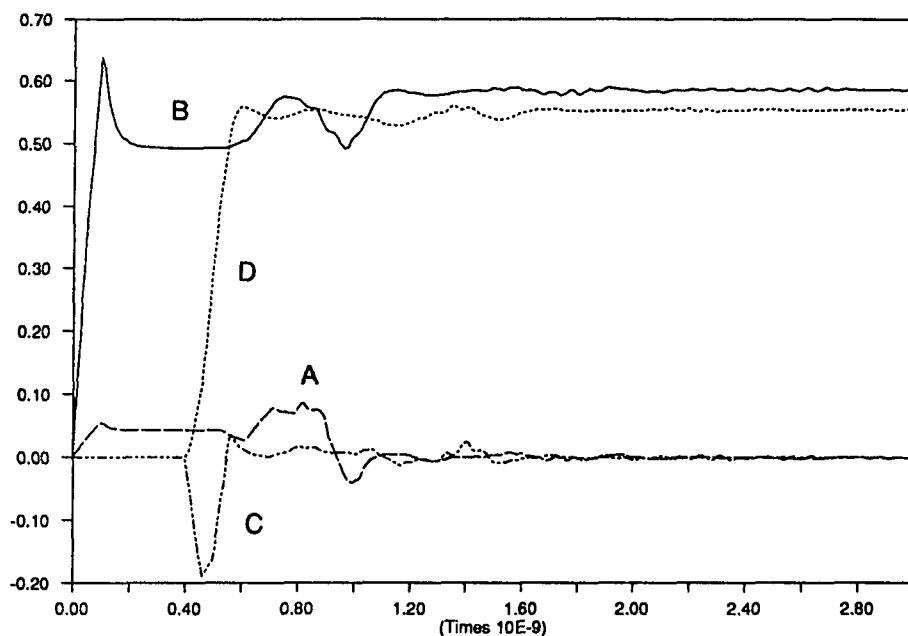


Fig. 5.2.3 The Transient Response calculated by LSPICE with $REL TOL=10^{-4}$;
A: Voltage at node 2; B: Voltage at node 3;
C: Voltage at node 11; D: Voltage at node 12.

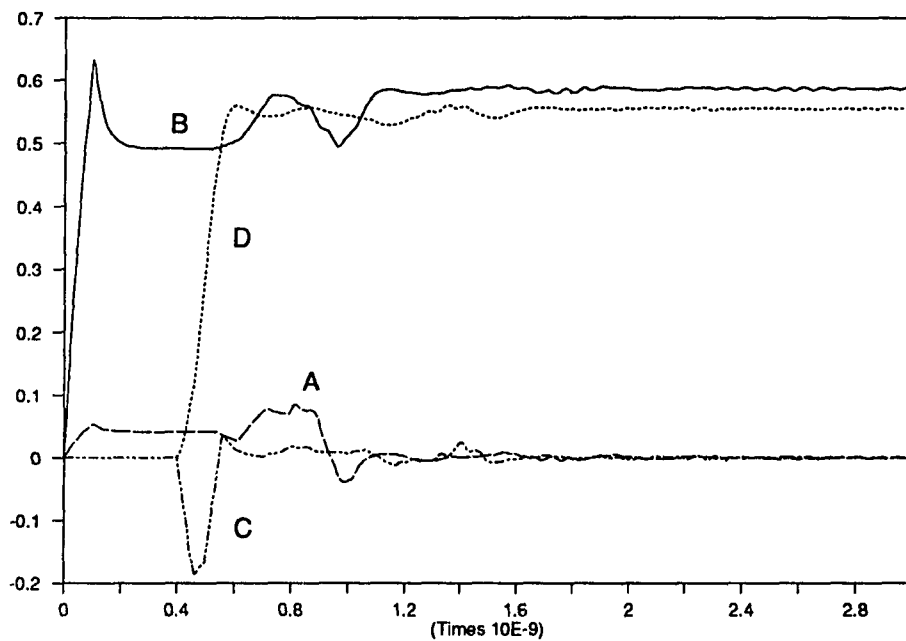


Fig. 5.2.4 The Transient Response calculated by UANTL with $ETOL=10^{-4}$;
A: Voltage at node 2; B: Voltage at node 3;
C: Voltage at node 11; D: Voltage at node 12.

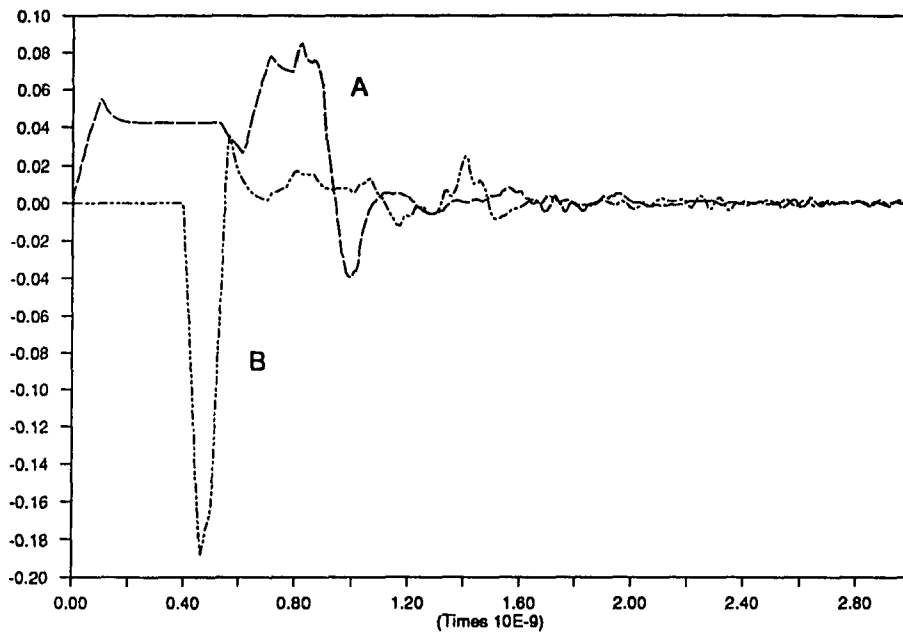


Fig. 5.2.5 The Transient Response calculated by LSPICE with $REL TOL=10^{-4}$;
A: Voltage at node 2; B: Voltage at node 11.

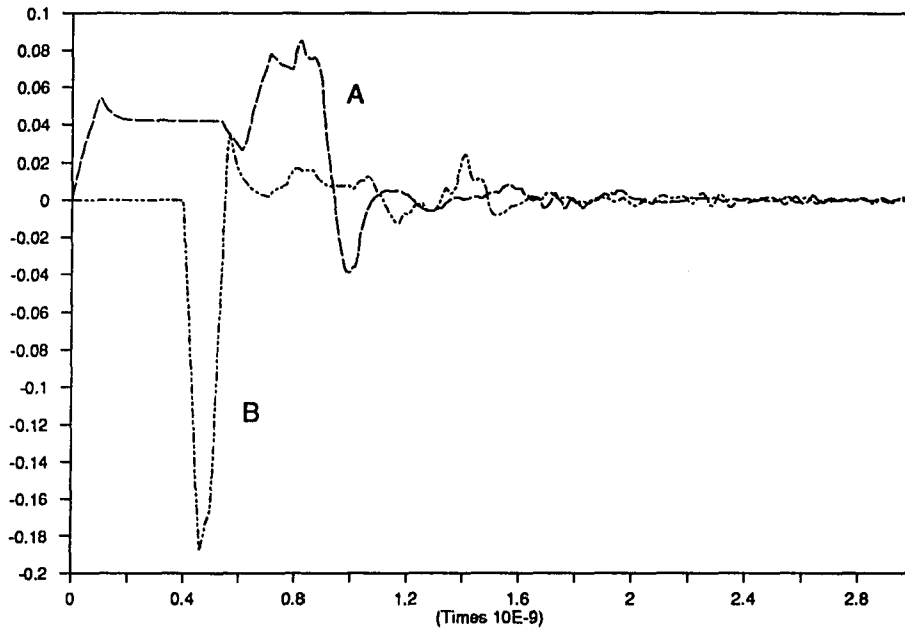


Fig. 5.2.6 The Transient Response calculated by UANTL with $ETOL=10^{-4}$;
A: Voltage at node 2; B: Voltage at node 11.

The CPU time required for the simulation with LSPICE and UANTL as follows:

LSPICE ($RELTOL=10^{-3}$) = 4709 sec

LSPICE ($RELTOL=10^{-4}$) = 4779 sec

UANTL ($ETOL=10^{-4}$) = 953 sec

Comparing the corresponding CPU time, we see that the saving of CPU time was yielded by using UANTL. LSPICE provides memory management to reduce the size of memory which is increased extensively by modal wave tracking. UANTL initially allocates memory space as a dimension. The initial allocation of fixed size of memory can save the CPU

time, but it waists memory space. The memory management is critical to simulate large number of circuit elements and transmission lines. LSPICE allocates memory whenever it is needed instead of initial allocation. It saves the memory space, but requires the CPU time overhead for memory management by separate memory allocations and memory movements. As shown by the results, the price to pay for the memory management is great when the number of transmission lines is increased.

For the purpose of comparison, the voltages at node 2 and node 11 obtained using LSPICE with $REL TOL=10^{-4}$ are used as reference values.

Table 5.2.1 Percentage Error of Voltage at Node 2
from the Reference Value.

Time (ns)	LSPICE RELTOL=10 ⁻⁴	LSPICE RELTOL=10 ⁻³		UANTL ETOL=10 ⁻⁴	
	(volt)	(volt)	% error	(volt)	% error
0.3	0.0425	0.0425	0.0	0.0423	0.5
0.6	0.0284	0.0284	0.0	0.0282	0.7
0.9	0.0478	0.0477	0.2	0.0482	0.8
1.2	0.0030	0.0030	0.0	0.0028	6.7
1.5	0.0037	0.0037	0.0	0.0038	2.7
1.8	-0.0009	-0.0010	1.1	-0.0009	0.0
2.1	-0.0013	-0.0013	0.0	-0.0013	0.0
2.4	0.0007	0.0007	0.0	0.0007	0.0
2.7	0.0012	0.0012	0.0	0.0011	8.3
3.0	0.0003	0.0003	0.0	0.0003	0.0

Table 5.2.2 Percentage Error of Voltage at Node 11
from the Reference Value.

Time (ns)	LSPICE RELTOL= 10^{-4}	LSPICE RELTOL= 10^{-3}		UANTL ETOL= 10^{-4}	
	(volt)	(volt)	% error	(volt)	% error
0.3	0.0000	0.0000	0.0	0.0000	0.0
0.6	0.0150	0.0152	1.3	0.0148	1.3
0.9	0.0084	0.0084	0.0	0.0088	4.8
1.2	-0.0073	-0.0073	0.0	-0.0077	5.5
1.5	-0.0069	-0.0070	0.1	-0.0065	5.8
1.8	-0.0015	-0.0015	0.0	-0.0015	0.0
2.1	0.0023	0.0024	4.3	0.0023	0.0
2.4	-0.0011	-0.0011	0.0	-0.0011	0.0
2.7	0.0004	-0.0004	0.0	-0.0004	0.0
3.0	0.0001	0.0001	0.0	0.0001	0.0

The differences among the results obtained using LSPICE and UANTL with same local truncation error settings are within 6.7 %. The differences are again due to the difference in the modal wave tracking algorithm.

5.3. Simulation of a Nonlinear Network with One Transmission Line

A network containing several nonlinear circuit elements and a two-conductor transmission line is shown in Fig. 5.3.1.

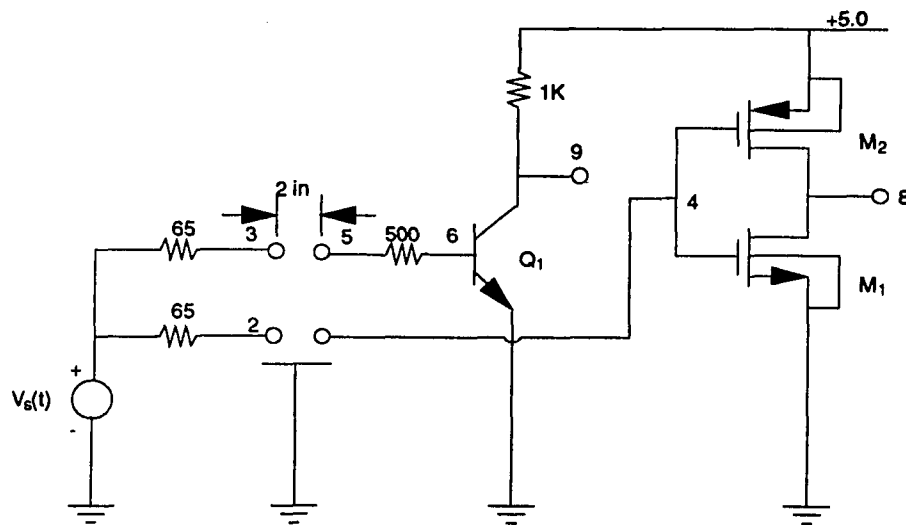


Fig. 5.3.1 A Nonlinear Network with One Transmission Line.

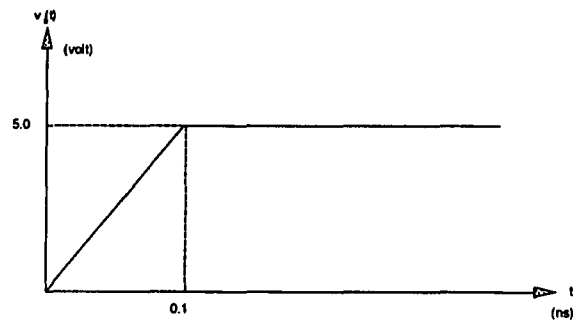


Fig. 5.3.2 Driving Voltage of the Network in Fig. 5.3.1.

The parameter values of transistor Q1, M1, and M2 in Fig. 5.3.1 are listed below.

BJT transistor Q1:

$$I_s = 1.0 \times 10^{-15} A$$

$$\beta_F = 100$$

$$\beta_R = 1.0$$

$$C_{JE} = 1.0 pF$$

$$m_{JE} = 0.33$$

$$V_{JE} = 0.6$$

$$C_{JC} = 3.0 pF$$

$$m_{JC} = 0.33$$

$$V_{JC} = 0.6$$

$$\tau_F = 0.1 nsec$$

$$\tau_R = 0.1 nsec$$

MOS transistors M1 and M2:

$$|V_{T0}| = 1.0$$

$$k = 1.0 \times 10^{-4}$$

$$\gamma = 0.37$$

$$\lambda = 0.0$$

$$2|\phi_F| = 0.6$$

$$I_s = 1.0 \times 10^{-15} \text{ A}$$

$$C_{BD} = 14.7 \text{ fF}$$

$$C_{BS} = 15.8 \text{ fF}$$

$$m_j = 0.33$$

$$C_{GDO} = 24.15 \text{ pF}$$

$$C_{GSO} = 24.15 \text{ pF}$$

The [L] and [C] matrices of the transmission line are

$$[L] = \begin{bmatrix} 3.792 & 0.836 \\ 0.836 & 3.792 \end{bmatrix}$$

$$[C] = \begin{bmatrix} 0.833 & -0.102 \\ -0.102 & 0.833 \end{bmatrix}$$

The units of [L] and [C] are $\frac{nF}{cm}$ and $\frac{pF}{cm}$ respectively.

The transient response of the network was simulated using LSPICE and UANTL with RELTOL set to 10^{-4} , ETOL set to 10^{-4} , respectively. The time interval of simulation is 3.0

nsec. The transients in these system were caused by the voltage source $V_s(t)$ changing in time as shown in Fig. 5.3.2. Voltages at node 2, node 3, node 8, and node 9 were plotted and are shown in Fig. 5.3.3, and Fig. 5.3.4.

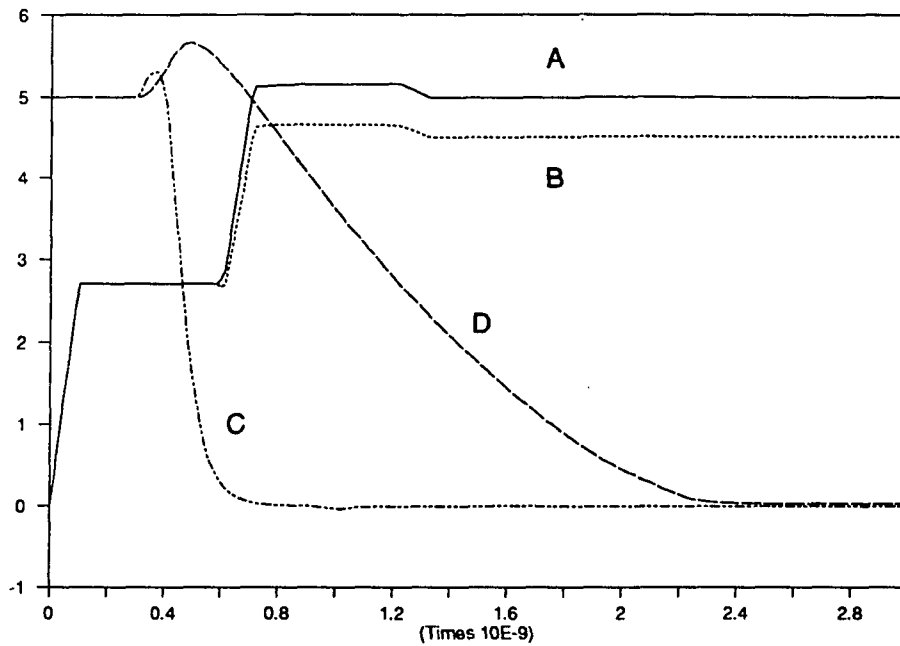


Fig. 5.3.3 Transient Response calculated by LSPICE with $RELTOL=10^{-4}$;
A: Voltage at node 2; B: Voltage at node 3;
C: Voltage at node 8; D: Voltage at node 9.

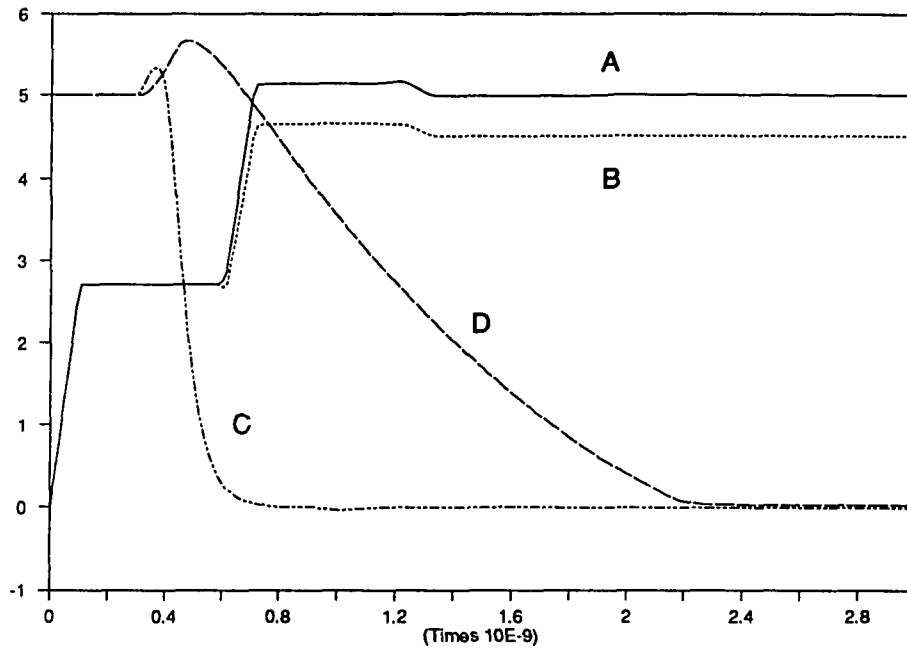


Fig. 5.3.4 Transient Response calculated by UANTL with $ETOL=10^{-4}$;
 A: Voltage at node 2; B: Voltage at node 3;
 C: Voltage at node 8; D: Voltage at node 9.

The CPU times required for simulation are listed below:

LSPICE (RELTOL= 10^{-3}) = 65 sec

LSPICE (RELTOL= 10^{-4}) = 69 sec

UANTL (ETOL= 10^{-4}) = 257 sec

As shown previous and section 5.1 results, the CPU times required for simulation in LSPICE are slight less or larger than in UANTL when the networks have a few the number of

transmission line system.

For the purpose of comparison, the voltages at node 8 and node 9 obtained using LSPICE with $RELTOL=10^{-4}$ are used as reference values. The percentage error from the reference values are calculated at some time points. The results are shown in Table 5.3.1, and Table 5.3.2. LSPICE is faster than UANTL because of more efficient handling of transistor models and longer ratio of the number of circuit nodes to the number of conductors in transmission lines.

Table 5.3.1 Percentage Error of Voltage at Node 8
from the Reference Value.

Time	LSPICE		UANTL		
	RELTOL= 10^{-4}	RELTOL= 2×10^{-3}	ETOL= 10^{-4}		
(ns)	(volt)	(volt)	% error	(volt)	% error
0.3	5.0000	5.0000	0.0	5.0000	0.0
0.6	0.2886	0.2826	2.1	0.2936	1.7
0.9	0.0043	0.0042	2.3	0.0046	7.0
1.2	-0.0024	-0.0024	0.0	-0.0026	8.3
1.5	0.0001	0.0001	0.0	0.0001	0.0
1.8	0.0002	0.0002	0.0	0.0002	0.0
2.1	0.0000	0.0000	0.0	0.0000	0.0
2.4	0.0000	0.0000	0.0	0.0000	0.0
2.7	0.0000	0.0000	0.0	0.0000	0.0
3.0	0.0000	0.0000	0.0	0.0000	0.0

Table 5.3.2 Percentage Error of Voltage at Node 9
from the Reference Value.

Time (ns)	LSPICE RELTOL= 10^{-4}	LSPICE RELTOL= 2×10^{-3}		UANTL ETOL= 10^{-4}	
	(volt)	(volt)	% error	(volt)	% error
0.3	5.0000	5.0000	0.0	5.0000	0.0
0.6	5.4020	5.4010	0.0	5.3440	1.1
0.9	4.0560	4.0550	0.0	3.9780	1.9
1.2	2.7940	2.7930	0.0	2.7240	2.5
1.5	1.7480	1.7470	0.1	1.6870	3.5
1.8	0.8904	0.8897	0.1	0.8429	5.3
2.1	0.2851	0.2846	0.2	0.2177	23.6
2.4	0.0359	0.0359	0.0	0.0317	11.7
2.7	0.0277	0.0277	0.0	0.0272	1.8
3.0	0.0262	0.0262	0.0	0.0261	0.4

The differences among the results obtained using LSPICE with different RELTOL settings are within 2.3 %. But, the maximum percentage error of UANTL, from the

$$[L] = \begin{bmatrix} 2.673 & 0.521 \\ 0.521 & 3.577 \end{bmatrix}$$

$$[C] = \begin{bmatrix} 1.304 & -0.0734 \\ -0.0734 & 0.896 \end{bmatrix}$$

The [L] and [C] matrices of transmission line #2 are

$$[L] = \begin{bmatrix} 4.196 & 1.185 & 0.478 \\ 1.185 & 4.143 & 1.185 \\ 0.478 & 1.185 & 4.196 \end{bmatrix}$$

$$[C] = \begin{bmatrix} 0.484 & -0.100 & -0.00972 \\ -0.100 & 0.509 & -0.100 \\ -0.00972 & -0.100 & 0.484 \end{bmatrix}$$

The units of [L] and [C] are $\frac{nH}{cm}$ and $\frac{pF}{cm}$, respectively.

The network was excited from the steady state by the voltage source indicated in Fig. 5.3.2 in section 5.3. The transient response of this network was simulated using LSPICE and UANTL for time interval of 2.0 nsec. Voltages at node 2, node 3, node 11, and node 15 were plotted and are shown in Fig. 5.4.2 and Fig. 5.4.3.

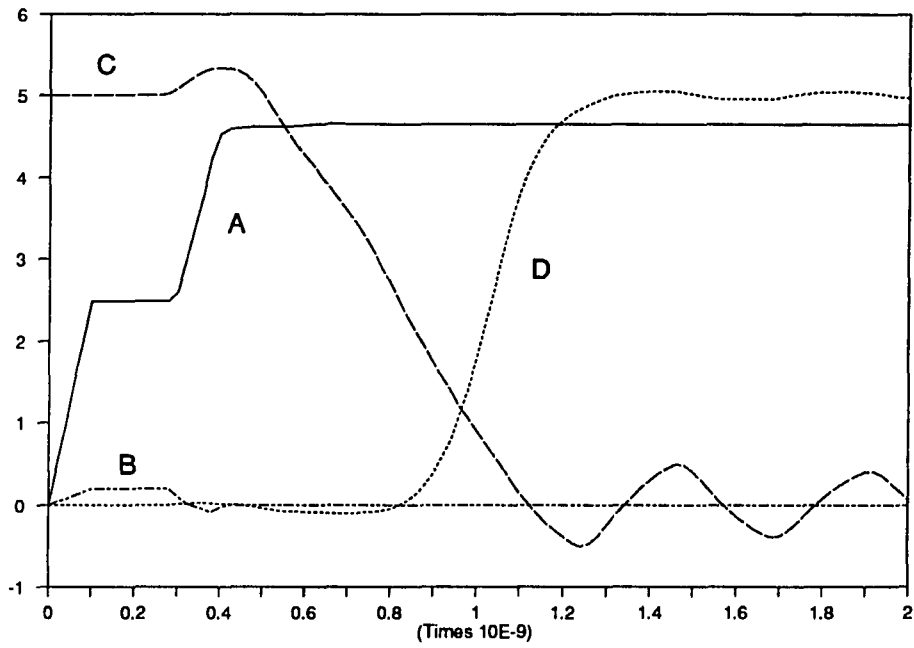


Fig. 5.4.2 Transient Response calculated by LSPICE with $RELTOL=10^{-4}$;
A: Voltage at node 2; B: Voltage at node 3;
C: Voltage at node 11; D: Voltage at node 15.

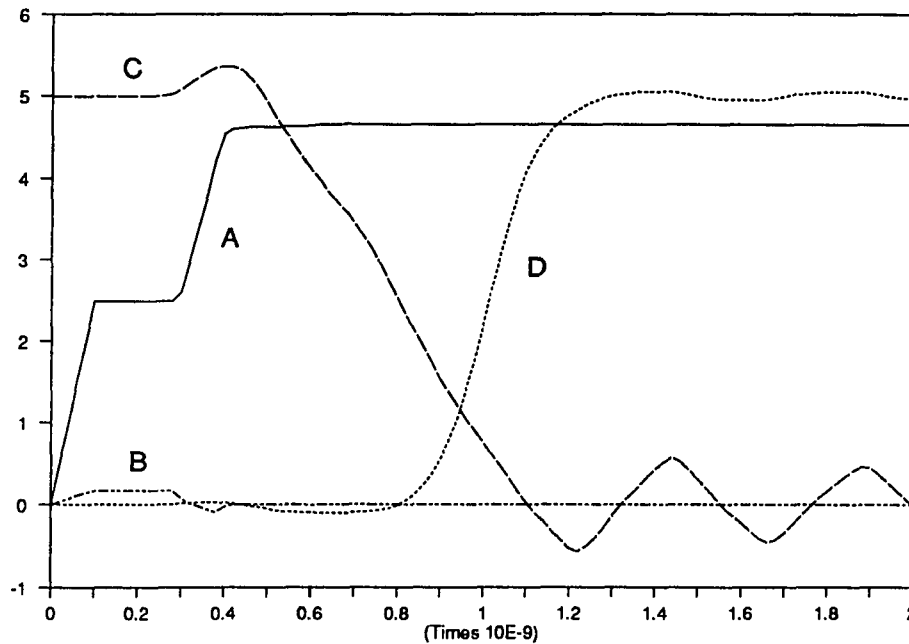


Fig. 5.4.3 Transient Response calculated by UANTL with $ETOL=10^{-4}$;
 A: Voltage at node 2; B: Voltage at node 3;
 C: Voltage at node 11; D: Voltage at node 15.

The CPU time required for the simulation are listed below:

LSPICE ($RELTOL=10^{-4}$)=3412 sec

UANTL ($ETOL=10^{-4}$)=1221 sec

The UANTL requires less CPU time for simulation of this example same as the results in section 3.3. The CPU time needed by LSPICE used grows rapidly when the number of transmission lines increase because of memory management.

For the purpose of comparison, the voltages at node 11 and node 15 obtained using

LSPICE with $\text{RELTOL}=10^{-4}$ are used as reference values. The percentage errors from the reference values are calculated at certain time points. The results are shown in Table 5.4.1, and Table 5.4.2.

Table 5.4.1 Percentage Error of Voltage at Node 11
from the Reference Value

Time (ns)	LSPICE RELTOL= 10^{-4}	LSPICE RELTOL= 10^{-3}		UANTL ETOL= 10^{-4}	
	(volt)	(volt)	% error	(volt)	% error
0.2	5.0000	5.0000	0.0	4.9990	0.0
0.4	5.3350	5.3350	0.0	5.3630	0.5
0.6	4.2480	4.2470	0.0	4.0950	3.6
0.8	2.6960	2.6960	0.0	2.5280	6.2
1.0	0.9050	0.9044	0.1	0.7081	21.8
1.2	-0.3913	-0.3919	0.2	-0.5277	34.9
1.4	0.3051	0.3058	0.2	0.4147	35.9
1.6	-0.1347	-0.1353	0.4	-0.2233	65.8
1.8	0.0790	0.0796	0.8	0.1545	95.6
2.0	0.0706	0.0700	0.8	-0.0022	103

Table 5.4.2 Percentage Error of Voltage at Node 15
from the Reference Value

Time (ns)	LSPICE RELTOL= 10^{-4}	LSPICE RELTOL= 10^{-3}		UANTL ETOL= 10^{-4}	
	(volt)	(volt)	% error	(volt)	% error
0.2	0.0000	0.0000	0.0	0.0000	0.0
0.4	0.0196	0.0196	0.0	0.0228	16.3
0.6	-0.0828	-0.0829	0.1	-0.0933	12.7
0.8	-0.0430	-0.0431	0.2	-0.0105	75.6
1.0	1.7800	1.7810	0.1	2.1890	23.0
1.2	4.7120	4.7120	0.0	4.7220	0.2
1.4	5.0450	5.0450	0.0	5.0530	0.2
1.6	4.9530	4.9530	0.0	4.9490	0.1
1.8	5.0390	5.0390	0.0	5.0440	0.1
2.0	4.9710	4.9710	0.0	4.9450	0.5

It can be noted that the results obtained using LSPICE with different RELTOL settings are almost same. But, the results obtained using UANTL with same local truncation

error show big differences at some time points with maximum value 75.6 % at the node 15 and 103 % at node 11. Whenever the modal wave tracking errors reached the other end, the nodal voltage error were amplified by the reflected waves. So, the modal wave tracking algorithm implemented in LSPICE is again proven to be more accurate than that of UANTL.

CHAPTER 6

CONCLUSIONS

The modules for processing of interconnection specifications which are provided in an input file of circuit analyzer were developed. A software package for creation of appropriate computer models on the basis of topology and library of network components was also constructed and implemented using SPICE program. SPICE numerical techniques and the modal analysis of coupled lossless transmission lines have been successfully combined together and implemented to provide an efficient method of simulating the transient response of networks containing coupled lossless transmission lines. Simulator input processing and interconnection equation generation program, called SIP, consists of modules which are used like library functions (utilizing a tool concept). An effort was made in writing this software package to obtain high computational efficiency because of anticipated strong demand for simulation of circuit and interconnections.

The LSPICE has several advantages over UANTL and SPICE in simulating the transient response of network containing coupled lossless transmission lines. First, it is much easier to prepare the input file for circuit with coupled transmission lines. Second, the algorithm of modal wave tracking method of LSPICE is more accurate than that of UANTL. It is very important to obtain a good control of accuracy in the simulation of networks with coupled transmission lines. Third advantage is the availability of sophisticated transistor models built into the program. These models are compatible with the ones used in engineering practice.

The LSPICE needs more CPU time than UANTL for simulating simple circuits with several coupled transmission line systems. With a large number of transmission line systems, the number of non-zero off-diagonal terms of characteristic admittance matrix increases rapidly, system matrix becomes dense, and the sophisticated sparse matrix algorithm implemented in SPICE inefficient. This dramatically increases the operation count for solving the nodal equation matrix. Also, LSPICE provides memory management to reduce the size of memory which is increased extensively by modal wave tracking. UANTL initially allocates memory space as a dimension. The initial allocation of fixed size of memory can save the CPU time, but it wastes memory space. The memory management is critical in simulating large number of circuit elements and transmission lines. LSPICE allocates memory whenever it is needed instead of initial allocation. It saves the memory space, but requires the CPU time overhead for memory management by separate memory allocations and memory movements. As shown by the examples, the price to pay for the memory management in terms of CPU time increases when the number of transmission lines increases. This difference between UANTL and LSPICE turns into opposite direction when terminating networks are more complicated and contain more transistors, which is often the case in practice.

Future work on LSPICE can be directed toward a change of the solution method to one based on a spectral technique (Palusinski, et al., 1989) to improve its CPU time. Since a lossy transmission line can be represented by the circuit model derived from the impulse response data, or transfer function method (Gruodis, et al., 1981), LSPICE can be expanded to incorporate the capability of simulating the transient responses of networks containing both lossless and lossy transmission lines.

APPENDIX A

INPUT FILES FOR EXAMPLES USED
IN NUMERICAL EXPERIMENTS

1. Input File for Linear Network with One Transmission Line.

```
THIS IS FOR TEST A TL LINE
R1 1 0 66.05
R2 3 0 66.05
R3 4 0 66.05
R4 5 0 66.05
Y1 2 4 T=1 N=1 D=300 L1=500P L2=300P C1=0.10P C2=-0.04P
Y2 3 5 T=1 N=2 L1=300P L2=500P C1=-0.04P C2=0.10P
VS 2 1 PWL (0 0 0.1N 2.0 )
.PRINT TRAN V(2) V(3) V(4) V(5)
.TRAN 0.02N 9N
.OPTION ACCT NODE LIST RELTOL=0.0001 LIMPTS=4501
.END
```

2. Input File for Linear Network with Two Transmission Lines.

```
THIS IS A LINEAR NETWORK CONTAINING TWO T.L
R1 1 0 65
C1 1 0 1.0P
R2 2 0 65
R3 4 0 65
R4 13 0 87
R5 12 0 87
C2 12 0 1.0P
R6 11 0 87
R7 5 8 5.0
R8 6 9 5.0
R9 7 10 5.0
Y1 2 5 T=1 N==1 D=0.0508 L1=0.3792U L2=0.0836U L3=0.0292U C1=0.0883N
+ C2=-0.0102N C3=-0.00779N
Y2 3 6 T=1 N=2 L1=0.0836U L2=0.3753U L3=0.0836U C1=-0.0102N
+ C2=0.0899N C3=-0.0102N
Y3 4 7 T=1 N=3 L1=0.0292U L2=0.0836U L3=0.3792U C1=-0.00779N
+ C2=-0.0102N C3=0.0883N
```

```

Y4 8 11 T=2 N=1 D=0.0254 L1=0.5033U L2=0.1734U L3=0.0818U
+      C1=0.0677N C2=-0.0163N C3=-0.00145N
Y5 9 12 T=2 N=2 L1=0.1734U L2=0.4972U L3=0.1734U
+      C1=-0.0163N C2=0.0722N C3=-0.0163N
Y6 10 13 T=2 N=3 L1=0.0818U L2=0.1734U L3=0.5033U
+      C1=-0.00145N C2=-0.0163N C3=0.0677N
VSS 3 1 PWL (0 0.0 0.1N 1.0 3N 1.0)
.TRAN 0.0075N 3N
.PRINT TRAN V(2) V(3) V(11) V(12)
.OPTION ACCT LIST NODE RELTOL=0.0001 ITL5=30000 LIMPTS=610
.END

```

3. Input File for Nonlinear Network with One Transmission Line.

```

THIS CIRCUIT IS A NONLINEAR NETWORK WITH T.L.
R1 1 2 65.0
R2 1 3 65.0
R3 5 6 500.0
R4 7 9 1K
Y1 3 5 T=1 N=1 D=0.0508 C1=0.0883N C2=-0.0102N L1=0.3792U L2=0.0836U
Y2 2 4 T=1 N=2 C1=-0.0102N C2=0.0883N L1=0.0836U L2=0.3792U
Q1 9 6 0 QMODE
.MODEL QMODE NPN IS=1.0F BF=100 BR=1.0 CJE=1.0P MJE=0.33 VJE=0.6
+ CJC=3.0P TF=0.1N TR=0.1N CJE=1.0P MJC=0.33 VJC=0.6
M1 8 4 7 7 MODE1
M2 8 4 0 0 MODE2
.MODEL MODE1 PMOS VTO=-1.0 KP=0.1M GAMMA=0.37 PHI=0.3 IS=1.0F
+ CBD=14.7F CBS=15.8F MJ=0.33 CGD0=24.15P CGS0=24.15P LAMBDA=0.0
+ KP=0.1M PB=0.6
.MODEL MODE2 NMOS VTO=1.0 KP=0.1M GAMMA=0.37 PHI=0.3 IS=1.0F
+ CBD=14.7F CBS=15.8F MJ=0.33 CGD0=24.15P CGS0=24.15P
+ LAMBDA=0.0 KP=0.1M PB=0.6
V1 7 0 DC 5.0
VSS 1 0 PWL (0 0 0.1N 5 3N 5)
.TRAN 0.015N 3N
.PRINT TRAN V(2) V(3) V(8) V(9)
.OPTION ACCT LIST NODE OPTS RELTOL=0.0001
.END

```

4. Input File for Nonlinear Network with Two Transmission Lines.

THIS CIRCUIT IS A NONLINEAR NETWORK WITH TWO T.L. SYSTEM

```

R1 1 2 45.3
R2 3 0 63.2
R3 5 0 63.2
R4 4 6 500
R5 7 8 1K
R6 9 0 93.1
R7 10 0 93.1
R8 13 0 93.1
R9 12 0 93.1
Y1 2 4 T=1 N=1 D=0.0254 C1=0.1304N C2=-7.34P L1=0.2673U L2=0.0521U
Y2 3 5 T=1 N=2 D=0.0254 C1=-7.34P C2=0.0896N L1=0.0521U L2=0.3577U
Y3 8 11 T=2 N=1 D=0.0254 C1=0.0484N C2=-0.0100N C3=-0.972P
+   L1=0.4196U L2=0.1185U L3=0.0478U
Y4 9 12 T=2 N=2 D=0.0254 C1=-0.0100N C2=0.0509N C3=-0.0100N
+   L1=0.1185U L2=0.4143U L3=0.1185U
Y5 10 13 T=2 N=3 C1=-0.972P C2=-0.0100N C3=0.0484N
+   L1=0.0478U L2=0.1185U L3=0.4196U
Q1 8 6 0 QMODE
.MODEL QMODE NPN IS=1.0F BF=100 BR=1.0 CJE=1.0P MJE=0.33 VJE=0.6
+   CJC=1.0P CJE=1.0P TF=0.1N TR=0.1N CJE=1.0P MJC=0.33 VJC=0.6
M1 15 11 14 14 MODE1
M2 15 11 0 0 MODE2
.MODEL MODE1 PMOS VTO=-1.0 KP=0.1M GAMMA=0.37 PHI=0.3 IS=1.0F
+   CBD=14.7F CBS=15.8F MJ=0.33 CGD0=24.15P CGS0=24.15P LAMBDA=0.0
+   KP=0.1M PB=0.6
.MODEL MODE2 NMOS VTO=1.0 KP=0.1M GAMMA=0.37 PHI=0.3 IS=1.0F
+   CBD=14.7F CBS=15.8F MJ=0.33 CGD0=24.15P CGS0=24.15P
+   LAMBDA=0.0 KP=0.1M PB=0.6
V1 7 0 DC 5
V2 14 0 DC 5
VSS 1 0 PWL (0 0 0.1N 5 2N 5)
.TRAN 0.02N 2N
.PRINT TRAN V(2) V(3) V(11) V(15)
.OPTION ACCT LIST NODE RELTOL=0.0001 LIMPTS=420 ITL5=50000
.END

```

APPENDIX B

COMMON STATEMENTS

```

COMMON /TABINF/ IELMNT,ISBCKT,NSBCKT,IUNSAT,NUNSAT,
1  ITEMS,NUMTEM ISENS,NSENS,IFOUR,NFOUR,IFIELD,
2  ICODE,IDELIM,ICOLUM,INSIZE,JUNODE,LSBKPT,NUMBKP,
3  IORDER,IMNODE,IUR,IUC,ILC,ILR,NUMOFF,ISR,
4  NMOFFC,ISEQ,ISEQ1,NEQN,NODEVS,NDIAG,ISWAP,IEQUA,
5  MACINS,LVNIM1,LX0,LVN,LYNL,LYU,LYL,LX1,
6  LX2,LX3,LX4,LX5,LX6,LX7,LD0,LD1,LTD,
7  IMYNL,IMVN,LCVN,NSNOD,NSMAT,NSVAL,ICNOD,ICMAT,
8  ICVAL,LOUTPT,LPOL,LZER,IRSWPF,IRSWPR,ICSWPF,
9  ICSWPR,IRPT,JCPT,IROWNO,JCOLNO,NTTBR,NTTAR,LVNTMP
COMMON /MISCEL/ ATIME,APROG(3),ADATE,ATITLE(10),DEFL,
1  DEFW,DEFAD,DEFAS,RSTATS(50),IWIDTH,LWIDTH,NOPAGE
COMMON /LINE/ ACHAR,AFIELD(15),OLDLIN(15),KNTRC,KNTLIM
COMMON /CIRDAT/ LOCATE(50),JELCNT(50),NUNODS,NCNODS,
1  NUMNOD,NSTOP,NUT,NLT,NXTRM,NDIST,NTLIN,IBR,
2  NUMVS,NUMALT,NUMCYC
COMMON /MOSARG/ VTO,BETA,GAMMA,PHI,PHIB,COX,XNSUB,
1  XNFS,XD,XJ,XLD,XLAMDA,UO,UEXP,VBP,UTRA,VMAX,
2  XNEFF,XL,XW,VBI,VON,VDSAT,QSPOF,BETA0,BETA1,
3  CDRAIN,XQCO,XQC,FNARRW,FSHORT,LEV
COMMON /STATUS/ OMEGA,TIME,DELTA,DELOLD(7),AG(7),VT,
1  XNI,EGFET,XMU,SFACTR,MODE,MODEDC,ICALC,INITF,
2  METHOD,IORD,MAXORD,NONCON,ITERNO,ITEMNO,NOSOLV,
3  MODAC,PIV,IVMFLG,IPOSTP,ISCRCH,IOFILE
COMMON /FLAGS/ IPRNTA,IPRNTL,IPRNTM,IPRNTN,IPRNTO,
1  LIMTIM,LIMPTS,LVLCOD,LVLTIM,ITL1,ITL2,ITL3,ITL4,
2  ITL5,ITL6,IGOOF,NOGO,KEOF
COMMON /KNSTNT/ TWOPI,XLOG2,XLOG10,ROOT2,RAD,BOLTZ,
1  CHARGE,CTOK,GMIN,RELTOL,ABSTOL,VNTOL,TRTOL,
2  CHGTOL,EPSO,EPSSIL,EPSOX,PIVTOL,PIVREL
COMMON /MEMMGR/ CPYKNT,ISTACK(1),LORG,ICORE,MAXCOR,
1  MAXUSE,MEMAVL,LDVAL,NUMBLK,LOCTAB,LTAB,IFWA,
2  NWOFF,NTAB,MAXMEM,MEMERR,NWD4,NWD8,NWD16
COMMON /DC/ TCSTAR(2),TCSTOP(2),TCINCR(2),ICVFLG,
1  ITCELM(2),KSSOP,KINEL,KIDIN,KOVAR,KIDOUT
COMMON /TRAN/ TSTEP,TSTOP,TSTART,DELMAX,TDMAX,FORFRE,JTRFLG
COMMON /AC/ FSTART,FSTOP,FINCR,SKW2,REFPRL,SPW2,JACFLG,IDFREQ,
1  INOISE,NOSPRT,NOSOUT,NOSIN,IDIST,IDPRT
COMMON /OUTINF/ XINCR,STRING(15),XSTART,YVAR(8),ITAB(8),
1  ITYPE(8),ILOGY(8),NPOINT,NUMOUT,KNTR,NUMDGT

```

```
COMMON /CJE/ MAXTIM,ITIME,ICOST  
COMMON /DEBUG/ IDEBUG(20)  
COMMON /BLANK/ VALUE(200000)  
INTEGER NODPLC(64)  
COMPLEX CVALUE(32)  
EQUIVALENCE (VALUE(1),NODPLC(1),CVALUE(1))  
PARAMETER (NTLSA=10, NTLA=20)  
COMMON /A/ VM(NTLSA,NTLA,NTLA), VMI(NTLSA,NTLA,NTLA)  
COMMON /B/ YGC(NTLSA,NTLA,NTLA)  
COMMON /C/ NTL, INL(NTLSA)
```

LIST OF REFERENCES

- Antognetti P., Massobrio G., "Semiconductor Device Modeling with SPICE", McGraw-Hill Book Company, 1988.
- Chang C. S., "Advances in CAD for VLSI", (Ruehli A. E., Ed.), in Transmission Lines, Amsterdam, The Netherlands, North-Holland, Pt. 2, pp. 292-332, 1987.
- Chang F. Y., "Transient Analysis of Lossless Coupled Transmission Lines in a Nonhomogeneous Dielectric Medium", IEEE Trans. on Microwave Theory and Tech., Vol. MTT-18, 616-626, Sep. 1970.
- Cohen E., "Program Reference for SPICE2", Electronics Research Laboratory Rep. No. ERL-M592, University of California, Berkeley, 1976.
- Gruodis A. J., Chang C. S., "Coupled Lossy Transmission Line Characterization and Simulation", IBM J. Res. Develop. Vol. 25, No. 1, Jan. 1981.
- Ho C. W., "Theory and Computer-Aided Analysis of Lossless Transmission Lines", IBM J. RES. DEV. 17, May, 1973.
- Liao J. C., "Computer Simulation of Multiple Coupled Transmission Lines in Electronic Packaging Application", Ph.D. Dissertation, University of Arizona, Tucson, Mar. 1989.
- Liao J. C., Palusinski O. A., Prince J. L., "Computer-Aided Analysis of Multiconductor Interconnections for VLSI Applications", Department of Electrical and Computer Engineering, The University of Arizona, Tucson, 1990.
- Nagel L. W., "SPICE2: A Computer Program to Simulate Semiconductor Circuits", Electronic Research Laboratory Rep. No. ERL-M520, University of California, Berkeley, 1975.
- Palusinski O. A., Liao J. C., Teschan P. E., Quintero F., "Electrical Modeling of Interconnections in Multilayer Packaging Structures", IEEE Trans. Components, Hybrid, Manuf. Technol., Vol. CHMT-10, No. 2, pp. 217-223, June 1987.
- Palusinski O. A., Lee A., "Analysis of Transients in Nonuniform and Uniform Multiconductor Transmission Lines", IEEE Trans. on Microwave Theory and Tech., Vol. 37, No. 1, Jan. 1989.
- Palusinski O. A., Liao J. C., Prince J. L., Cangellaris A. C., "Simulation of Transients in VLSI Packaging Interconnections", IEEE Trans. on Components, Hybrids, and Manufacturing Tech., Vol. 13, No. 1, Mar. 1990

Ruehli A. E., "Interface Calculation in a Complex Integrated Circuit Environment", IBM J. Res. Develop., pp. 470-479, Sep. 1972.

Ruehli A. E., "Circuit Analysis, Simulation and Design", Elsevier Science Publishers B. V., North Holland, 1986.

SPICE Version 2G User's Guide.

SPICE2 version 2G6, Department of Electrical Engineering and Computer Science, University of California, Berkeley, CA. 94720.

Weeks W. T., "Calculations of Coefficients of Capacitance of Multiconductor Transmission Lines in the Presence of a Dielectric Interface", IEEE Trans. Microwave Theory and Tech., MTT-18, 35-43, 1970.